THE DEVELOPMENT OF ENERGY-ABSORBING DEVICES FOR ASEISMIC BASE ISOLATION SYSTEMS

by

James M. Kelly
Professor of Civil Engineering

and

D. F. Tsztoo
Graduate Student

Division of Structural Engineering
and Structural Mechanics

Report No. UCB/EERC-78/01
Earthquake Engineering Research Center
College of Engineering
University of California
Berkeley, California
January, 1978

10

ABSTRACT

This report describes the behavior of mild steel energy-absorbing devices that can be used in earthquake isolation systems. The devices are rigid under service-type loading, but yield and absorb energy under large earthquake-type loading. The devices were shown to have substantial hysteretic energy abosrbing capacity over a useful life in excess of 300 cycles, far exceeding any load duration which can be expected from earthquake loadings. The hysteresis loops developed by sinusoidal loading of the devices effectively bounded the loops obtained by the random loading of the devices. The actual incorporation of the devices in a structural steel frame is being investigated in ongoing research.

ACKNOWLEDGEMENT

The research reported herein was supported by National Science Foundation Grant ENV 76-04262-A02.

TABLE OF CONTENTS

I INTRODUCTION

We describe a series of tests designed to determine favorable characteristics for an energy-absorbing device to be used in conjunction with a base isolation system. The devices were to have high initial elastic stiffness, flat post-yield response and high damping capacity; they were to be reliable and their response predictable. The devices are designed to act as mechanical fuses in that they are rigid under small excitations such as wind loading or small earthquake motions, but yield under large loading and thus dissipate energy. The advantages of incorporating these devices into a base isolation system are that damage would be concentrated in replaceable elements and the devices, being mechanical, would require little or no maintenance.

Two energy-absorbing devices both based on the plastic torsion of mild steel bars were tested to determine: (1) cyclic response, capacity to dissipate energy and fatigue life under displacement-controlled sinusoidal loading at various rates, (2) response and fatigue life under random loading and (3) the influence of device geometry on response.

Devices of the type described here have been used in shaking table experiments on a stepping frame [1] and on a frame on a rubber base isolation system [2,3,4]. Devices based on the model are being used in a railway bridge under construction in New Zealand. The purpose of this report is to describe the development preceding the application of these devices to the shaking table experiments.

In the application to the stepping frame [1] the devices operate in a vertical direction. The column foot of the stepping frame is free to uplift vertically, restrained only by the device; when the column foot moves off the base the device produces a downward restraining force and when the foot moves downwards the inelastic response of the device produces an upward force on the column foot. In the rubber bearing foundation system the action of the device is horizontal.

II DEVICES, INSTRUMENTATION AND TESTING PROCEDURE

Based on the results of an earlier feasibility study [5,6], the following design criteria were established for the energy-absorbing devices:

(1) The principal mechanism of energy absorption should be torsional plastic deformation.

(2) The devices should be fabricated from a material capable of sustaining high levels of plastic deformation and hysteretic damping.

(3) The devices should have sufficient integrity to function after undergoing a great many loading cycles.

(4) The devices should be fabricated easily and economically.

These requirements were met by a design incorporating a mild steel torsion bar of rectangular cross section. Such a cross section was chosen to facilitate external clamping of the device to fixtures or interfaces and to limit device deterioration. The externally applied torque is transferred to the torsion bar by means of moment arms or clamps. Outer clamping arms fix the torque action and integrate the device with structural and/or foundation elements. A set of inner arms coupled to active elements of the frame twists the bar when any of the active elements are displaced. As a result of the preliminary investigation, the connections chosen for the energy-absorbing device were 3/8" fillet welds. Two device configurations as illustrated in Figures 1 and 2 were tested. It is important to note that the welding was done on the outside of the outside bars and the inside of the inside bars (Figures 1 and 2). This welding arrangement was found in the earlier research to be particularly efficient in that the torque is transmitted to the bars through surface contact and not through the welds themselves, thus inhibiting weld failure.

Type A devices were flat in appearance with centerlines of symmetry. The outer arms were drilled to accept 3/4" [1.91 cm] diameter high-strength bolts to hold the devices in the testing frame. The inner arms were drilled to accept 1" [2.54 cm] diameter high-strength pins through which the devices were externally loaded. Type A devices were tested under sinusoidal loading to assess the feasibility of the design and to establish that failure of the devices took place as required in the torsion bar and not in the welds. These devices were tested at a variety of loading rates under sinusoidal loading to assess the influence of rate on the response and life of the devices. Nonsinusoidal loading including random and periodic inputs was used to study initial yielding, torsional load capacity, cyclic deterioration and displacement versus force hysteresis with the purpose of developing an interrelation between the response under sinusoidal loading and that under random-type loading typical of earthquake motions.

Type B devices were tested to ascertain the effects of changing device configuration. Type B devices had an oblique rather than the flat geometry of the type A devices. The inner arms were distorted to provide freer access to the pin location and to facilitate attachment of the devices to structural elements. Device types A and B were physically similar in all other respects and, with the exception of the initial sinusoidal loading tests of device type A to establish the basic viability of the design and the periodic random loading tests described in Section IV of this report, were subjected to identical loading tests.

The devices were tested in a specially designed loading rig with a 50-kip [18650-Kg] capacity hydraulic ram operating in a displacement-controlled mode. The inner moment arms of the devices were stroked through nominal displacements of ±1/8", ±1/4", ±3/8", ±1/2", ±5/8", or ±3/4 [±.32 cm, ±.63 cm, ±.95 cm, ±1.27 cm, ±1.59 cm or ±1.91 cm] at the pin location with respect to the fixed outer arms. The forces corresponding to the displacement history were measured by a load cell and recorded by a data acquisition system.

The stroke displacement was applied in two ways as shown in Figure 3. Symmetric loading with the stroke centered about zero displacement was used to study hysteresis symmetry. Asymmetric loading with an input stroke offset by 0.1" and 0.2" [.25 cm and .51 cm] to bias the stroke in one direction (i.e. -.4" to +.6" or -.3" to +.7") was used to check any change in the shape of the hysteresis loops and to simulate field conditions where asymmetric loading might be expected.

In all tests the horizontal pin displacement of the device was recorded by means of a Linear Variable Displacement Transducer (LVDT) positioned opposite the pin location to measure actual horizontal displacements (Figure 4). Voltage data from the LVDT were fed through an amplifier and then recorded on a variety of systems including XY plotters and the low-speed Portable Nova Mini-Computer for the sinusoidal loading tests (Figures 5 and 6) or on the magnetic tape system of the high-speed Kinemetrics Data Acquisition System for the random loading tests (Figure 7).

In later tests horizontal displacements of the top and bottom of the torsion bar as well as pin displacements were recorded. As illustrated in Figure 8, two LVDT's were positioned opposite to the center of the torsion bar to measure displacements and to allow a study of angular rotation. Voltage data from these LVDT's were amplified and recorded in the manner described for the pin displacements (Figure 6). These bar displacements were recorded and plotted against pin displacements in the sinusoidal loading tests.

A load cell mounted on the horizontal ram of the testing frame was used to measure the force necessary to produce any corresponding horizontal displacement of the pin position (Figures 4 to 7). The load cell voltage data were passed through a control console calibration and recorded on XY plotters or on the acquisition systems previously described. Force was usually recorded and plotted instantaneously against either pin displacement or a time scale generated by a ramp generator during the sinusoidal loading tests. During the random loading tests the data were recorded but not plotted. Data reduction and processing for these tests were completed later.

During selected sinusoidal loading tests post-yield strain gages were applied to the open faces of the torsion bar to measure torsion and bending strains. Torsion was taken about the center of the 2" [5.18 cm] square face and bending at each corner in order to study strain distribution over the face of the torsion bar and to enable an assessment of the relative magnitudes of torsion and bending and the contribution of each to device hysteresis. The data from these tests were stored on separate channels of the Nova Mini-Computer and later analyzed and plotted.

III TESTING UNDER SINUSOIDAL LOADING

Device Hysteresis

The basic viability of the design of the energy-absorbing device having been established by preliminary testing, device types A and B were subjected to sinusoidal loading to study device hysteresis in detail. A study of the progressive behavior of the devices, from initial response at loading through cyclic deterioration and including assessments of physical torsion and bending behavior, was undertaken.

The sinusoidal wave was generated by a variable voltage generator with ±10-volt maximum range and a variable offset control to shift the voltage output to achieve various strokes and offsets. The voltage output was interpreted by a control console to obtain desired stroke displacements by means of the hydraulic loading ram testing rig. Maximum voltage amplitudes ranged from ±1.25 to ±5 volts with offsets of 0.0, 0.1 or 0.2 volts and frequencies from 1×10^{-4} to 400×10^{-4} Hz. Stroke displacements included ±1/4", ±3/8", ±1/2", ±5/8" and ±3/4" [±.63 cm, ±.95 cm, ±1.27 cm, ±1.59 cm and ±1.91 cm].

The initial pin displacement versus force hysteresis loops for device types A and B are shown in Figures 10a and 10b, respectively. The average elastic slope of the loops and yielding varied as shown in Table 1. The data in Table 1 were confirmed for both forward and backward displacements. Whereas the yield strength of the specimens was identical, the torsional stiffness increased substantially especially for the type B devices with their shorter effective moment arms. In Table 2, data on typical load capacity of the devices in the first few load cycles after yielding are given for the ±1/2" [±1.27 cm] displacement stroke tests. Similar data were obtained for tests with strokes of ±5/8" and ±3/4" [±1.59 cm and ±1.90 cm]. The force displacement curves for all type A devices were symmetric, but due to the oblique inner arms of the type B devices there was a 3 to 4 ratio in peak forward and backward forces. A decrease of 1" [2.54 cm] in the effective length of the inner moment arms substantially increased the force level.

The effect of strain hardening on device response was generally to increase force with increasing displacement (Figures 10a and 10b). However, the geometry of the type B device produced a response which in the backward direction has a more steeply rising character than in the forward direction. In fact, the interaction of the geometry and the natural strain hardening of the material produced a force displacement curve which is very nearly flat in the forward direction. In no other case did the force level decrease in the plastic region. Because the asymmetrical type B device was designed for use in a stepping frame [1], it was thought to be essential that the force-displacement characteristics of the device under asymmetric loading be established. Type B devices were therefore subjected to asymmetric loading with offsets of 0.1" and 0.2" [.25 cm and .51 cm] resulting in strokes of from -.4" to +.6" and from -.3" to +.7" [-1.07 cm to +1.52 cm and -.76 cm to +1.78 cm], respectively. These offsets generally produced no substantial change in the hysteresis loops from that shown in Figure 10b for a stroke of $\pm$1/2" other than the effect of the offset. The general shape and curvature of the loops were identical for all practical purposes as long as the total stroke range remained fixed at 1" [2.54 cm]. Only when the total stroke range was changed or when one direction of load failed to strain into the plastic range was there any significant difference in results. It was therefore concluded that results from symmetric loading tests could be extrapolated for asymmetric applications for the type B device.

Bar rotation and displacement were measured by means of LVDT's positioned at the top and bottom edges of the torsion bar. Data gathered from these instruments indicated that rotation had occurred about the top of the bar in both devices types. The greatest distortion was at the bottom portion of the torsion bar and fatigue cracking initiated from that location. During fatigue testing, type B devices accumulated a permanent deformation in the pointed direction of the oblique arms. After bringing the devices back to their initial zero pin displacement and force position, this deformation was approximately 1/4" [.63 cm] (Figure 11) when loading exceeded 300 cycles. Type A devices sustained no permanent deformation, a difference in response attributable to the differences in configuration of the two device types.

Measurements of strain from the faces of the torsion bars confirmed the observation of rotation about the top of the bars. Bending strains were greater in the bottom portion of the bar than in the top for both types of device. Torsional strains, isolated from bending strains, were almost linear with respect to pin displacement (Figure 12). The maximum bending and torsional strains were of comparable magnitude, not exceeding 2.5% for a stroke of ±1/2" [±1.27 cm]. Although total strain in combined torsion and bending was not measured, previous analysis by Kelly, Skinner and Heine [5] indicated that strains greater than 3.75% can be expected. Although the gages used in the present testing may not have been positioned properly to measure peak strain, the indicated maximum values may be taken as reliable estimates of the plastic strain developed in the material.

Typical pin displacement versus force hysteresis curves after initial cyclic hardening had occurred in both types of device are shown in Figures 13a and 13b. The outline of the hysteresis loops is similar, with both sets of loops passing through two nodes at approximately zero force. Force decay versus force plots for the two types of device are similar (Figures 14a and 14b). Decay was very gradual. Four decay stages can be distinguished: rapid initial loss of force capacity, degradation prior to cracking, force necking during crack development, and degradation after cracking.

After longitudinal cracks had developed in the torsion bar, the peak force steadily decreased with increasing cycle. However, as the peak force diminished the rate of decrease lessened, presumably due to the fact that the primary cause of the deterioration was the dissipation of energy and/or cumulative plastic work. If this is the case, the asymptotic decay curve would be negatively exponential. It is thus difficult to speak of the life of such devices and the term half-life becomes valuable. Thus, comparisons in the present work are made in terms of the half-life, i.e. the number of cycles at which the peak force is half its initial value. In general, the tests were terminated when this number of cycles had passed.

Progressive crack development was observed in the type B devices and to a lesser extent in the type A devices under sinusoidal loading (Figure 15). Cracking initiated at the bottom edge of the torsion bars at the interface between the bars and the inner torque arms. A similar set of cracks frequently developed at the outer arms after the inner cracks had progressed into the center portion of the bar. Although earlier cracking may have occurred, cracks were first observed between 50 and 90 loading cycles. The cracks generally progressed upward to the central portion of the bar and then longitudinally towards the center of each open face of the devices. As loading continued, the cracks developed through the cross section of the bar. The final cracking pattern of the type B devices (Figure 16) was similar to that for the type A devices. Although crack development was substantial, the devices retained approximately one-half their original damping capacity after about 400 cycles of sinusoidal loading.

Effect of Loading Rate

Type A devices were subjected to sinusoidal loading with pin displacements of ±3/8", ±1/2" and ±5/8" [±.95 cm, ±1.27 cm and ±1.59 cm] at loading rates of 0.02, 0.2 and 1.0 Hz to assess the influence of loading rate on device hysteresis and lifetime. The loading capacity of the hydraulic testing ram decreased with increasing loading rate, limiting the loading frequency to 1.0 Hz. The long-time fatigue response of the type A devices at higher rates was in every case found to be comparable to that of the devices at lower rates and in some cases was enhanced. It is difficult to draw conclusions about the long-time fatigue response of the device from these results since variations in welding from device to device resulted in considerable scatter in the fatigue life data. However, the results on rate effects appear to indicate that the damage to the devices is no greater at frequencies which are more typical of earthquakes than those at which the bulk of the testing was carried out.

IV TESTING UNDER NONSINUSOIDAL LOADING

Types A and B energy-absorbing device were subjected to nonsinusoidal loading in order to establish the energy-absorbing capacity and lifetime of the devices when input motion more characteristic of earthquake loading was used. Two series of tests were conducted. In the first series, both types of device were subjected to random nonperiodic wave forms (Figure 18), and in the second, type A devices were subjected to a set of recurring random wave forms with a period of 51.5 seconds (Figure 19). The wave forms were generated by a noise function generator with a ±10-volt range and a 2-Hz bandwidth. No offset adjustment was made. The nonperiodic function was used to study device response to random loading with nominal strokes of ±1/2", ±5/8" and ±3/4" [±1.27 cm, ±1.59 cm and ±1.91 cm]. The periodic function was used to study device deterioration over a number of loading cycles with nominal strokes of ±1/8", ±1/4" and ±1/2" [±.32 cm, ±.63 cm and ±1.27 cm]. All random voltage input was passed through a 2-Hz filter to allow stable interpretation by the control console and to simulate natural structural damping. The maximum voltage amplitude ranged from ±1.25 to ±4.00 volts with a variety of control console and amplifier calibrations to achieve the desired stroke displacements.

Nonperiodic Random Loading

Typical pin displacement versus force hysteresis and force or energy absorption capacity are shown in Figures 20 and 21. Device yielding and plasticity were not rigorously identified although both obviously occurred during peak displacement amplitudes. The first three seconds of device response is shown in Figure 20 and an assessment of lifetime damping capacity in Figure 21. The process of deterioration of the energy-absorbing capacity of the devices was not clear from the results of these tests. In an attempt to clarify this process, the loading input was intermittently stopped, the device subjected to a cycle of sinusoidal loading and device response recorded. By this procedure it was determined that although device deterioration and loss of energy-absorbing capacity had occurred under random loading, the devices had retained satisfactory levels of damping capacity and were able to endure prolonged cyclic loading. In Figures 22a and 22b, typical pin displacement versus force hysteresis loops are shown for five-second durations when a nominal stroke displacement of ±1/2" [±1.27 cm] was used. Results obtained using shorter displacement strokes were similar but proportionally smaller. In Figures 22a and 22b the approximate outline of the corresponding hysteresis loop for sinusoidal loading but otherwise identical testing conditions is indicated by a dashed line. A fair correlation exists between the response of the devices to sinusoidal and random loading in that the hysteresis loops for random loading are bound by those for sinusoidal loading. The effect of changing device geometry is apparent when the figures are compared. The 1" [2.54 cm] shorter effective torque arm of the type B device produced higher forces since the torque associated with the torsion bar remained essentially the same for both types of device. The oblique position of the inner torque arms of the type B device accounted for most of the asymmetry of peak load associated with this device.

Periodic Random Loading

Because it was difficult to define the deterioration of the devices under random loading with any precision, a series of tests were conducted under periodic random loading. When nonperiodic inputs were used, it was not possible to isolate device deterioration from the effects of the nonrepetitive input. The procedure adopted during the initial random loading tests, i.e. that of intermittently stopping the input to check device damping capacity by inputting a cycle of sinusoidal loading and recording the resulting hysteresis, did not provide sufficiently accurate results. By using random input that was periodic in that a random input function was repeated every 51.5 seconds, it was possible to study the hysteretic behavior of the devices in terms of the number of loading periods. The periodic random input used in these tests is shown in Figure 19; the function had a period of 51.5 seconds and for most tests a nominal amplitude of ±2 volts with scattered peaks slightly exceeding this value.

Since the changes in behavior introduced by the changes in geometry of the type B device had been shown to be predictable, only type A devices were tested under periodic random loading. In Figure 23 a group of hysteresis loops selected from 90 loading periods is shown, where each loop represents approximately 3.2 seconds of response taken 24 seconds after the beginning of the repeating loading period. Over the 90 loading periods -- 77 continuous minutes of testing -- the hysteresis loops closed significantly. Normal load capacity diminished from ±6 kips [±2238 Kg] to ±3 kips [±1119 Kg] and the energy-absorbing capacity as defined by the area enclosed by all loops dropped to approximately 1/3 to 1/2 of the original capacity by cycle 90.

The relationship between device response to sinusoidal and random loading is illustrated in Figure 24. For the same ±1/2" [±1.27 cm] nominal stroke displacement and device condition, the hysteresis loop for sinusoidal loading (shown in dashes) effectively bounded that for periodic random loading with the actual force capacity of the device at peak loading slightly underestimated. Nominal force decay over the 90 loading periods is more clearly shown in Figure 25. Rapid initial force necking was followed by a gradual decline in force. Overall, the decay of nominal force was similar to that for sinusoidal loading (compare Figures 14a and 14b to Figure 25). Crack propagation was also similar for the two types of loading. The final cracking pattern of the type A devices was brittle and jagged (Figure 26). Cracking along the longitudinal axis of the torsion bar was noted by the 25th period, having initiated from the bottom edge of the bar as noted in previous tests. By period 80, some cracks had worked completely through the bar cross section in numerous places along the longitudinal axis and cracking from the top edge of the bar had begun. Even in its half-life state, however, the device had substantial load damping capacity, approximately half that originally available.

V CONCLUSIONS

The testing program described herein established that the energy-absorbing devices whose design was based on the feasibility study by Kelly, Skinner and Heine [5,6] can operate under random loading typical of that which occurs during earthquakes.

Influence of Asymmetric Loading

When results from tests using identical sinusoidal stroke displacement amplitudes but differing pin displacements are compared, asymmetric loading is seen to effect hysteretic behavior negligibly except in that offset changes are reflected. So long as plastic behavior in both forward and backward displacement directions was achieved, the shape of the resulting hysteresis loops was unchanged and the damping capacity of the devices undiminished.

Influence of Changes in Device Geometry

Yielding in the torsion bar of the devices was not greatly affected by changes in device geometry under sinusoidal loading and may primarily depend on the properties of the mild steel bar used to fabricate a given device. On the other hand, device loading or damping capacity increased when shorter or out-of-plane inner moment arms were used. It would thus be possible to optimize device hysteresis for particular applications by alterations in design. Differential force capacity could be provided by using oblique inner arms where pin displacement or uplift might be expected to be greater in one direction than in another. Such changes in geometry also produce a relatively stiffer design against torsion produced by small elastic pin displacements which might be useful if a minimum system stiffness were required to resist pin displacement or base level uplift during normal service loading.

Bending versus Torsion and Crack Development

Bar rotation about the top edge of the torsion bar resulted in substantial energy absorption by bending as well as by torsion. Strain gage measurements indicated that peak bending and torsional strains were of comparable magnitude. Since the bar rotation was asymmetric about the top of the bar, cracking initiated from the bottom edge and worked up through the bar cross section. Rather than developing straight to the top edge of the bar, however, the cracks diverted along the longitudinal axis of the bar. Substantial hysteretic capacity thus remained even during advanced stages of crack development. In addition, the half-life of the devices is an order of magnitude greater than the number of critical loading cycles that would be expected during an earthquake.

Influence of Random Loading

Device hysteresis was also defined under random loading. Peak displacement-force responses and nominal force decay over periods of random loading were comparable to results obtained for sinusoidal loading. Lifetime deterioration for both types of loading was gradual and the half-life of the devices far exceeded any expected duration of damaging earthquake excitation. Although the devices can be replaced when damaged, the favorable results of the random loading tests suggest that it may be possible to design the devices to have a lifetime equal to that of the structures in which they are installed, especially if the devices are expected to be torqued only infrequently into the inelastic range by high-intensity earthquakes.

Basis for Design

Comparisons of the hysteresis loops for sinusoidal and random loading tests indicates a relationship between the two types of response. For the same stroke displacement and device condition, the hysteretic response of the devices for random loading was for the most part bounded by that for sinusoidal loading. This suggests a design procedure wherein device load or damping capacity is specified by first prescribing pin displacements or uplifts and then using sinusoidal loading inputs to check such designs, bearing in mind that the hysteretic response for sinusoidal loading may be a lower bound on peak hysteretic response for random loading. Reasonable safety factors may also be applied to the data obtained for sinusoidal loading to rate device damping capacity.

REFERENCES

[1] J. M. Kelly and D. F. Tsztoo, "Earthquake Simulation Testing of a Frame with Energy-Absorbing Devices," Report No. UCB/EERC-77/17, Earthquake Engineering Research Center, University of California, Berkeley, 1977.

[2] J. M. Kelly and J. M. Eidinger, "Earthquake Isolation Systems - Experimental Results," Proceedings of the Sixth Canadian Congress of Applied Mechanics, May 29 - June 3, 1977, pp. 295-296.

[3] C. J. Derham, et al., "Natural Rubber Foundation Bearings for Earthquake Protection - Experimental Results," Natural Rubber Technology, Vol. 8, Part 3, 1977, pp. 41-68.

[4] J. M. Kelly, J. M. Eidinger and C. J. Derham, "A Practical Soft Story Earthquake Isolation System," Report No. UCB/EERC-77/27, Earthquake Engineering Research Center, University of California, Berkeley, 1977.

[5] J. M. Kelly, R. I. Skinner and A. J. Heine, "Mechanisms of Energy Absorption in Special Devices for Use in Earthquake Resistant Structures," Bulletin of the New Zealand Society for Earthquake Engineering, Vol. 5, No. 3, September 1972, pp. 63-88.

[6] R. I. Skinner, J. M. Kelly and A. J. Heine, "Hysteretic Dampers for Earthquake-Resistant Structures," Earthquake Engineering and Structural Dynamics, Vol. 3, 1975, pp. 287-296.

TABLE 1 AVERAGE ELASTIC SLOPE OF LOOPS AND YIELDING - SINUSOIDAL LOADING TESTS

DEVICE TYPE	ELASTIC SLOPE	YIELDING
A	48 kip/in	4.0 kips
B	90 kip/in	4.6 kips

NOTE: 1 kip/in = 147 kg/cm
1 kip = 373 kg

TABLE 2 LOAD CAPACITY OF DEVICES AFTER INITIAL YIELDING - SINUSOIDAL LOADING TESTS - ±1/2" [±1.27 cm] STROKE

DEVICE TYPE	PEAK FORCE	
	BACKWARD	FORWARD
A	-6.0 kips	+6.0 kips
B	-11.0 kips	+8.0 kips

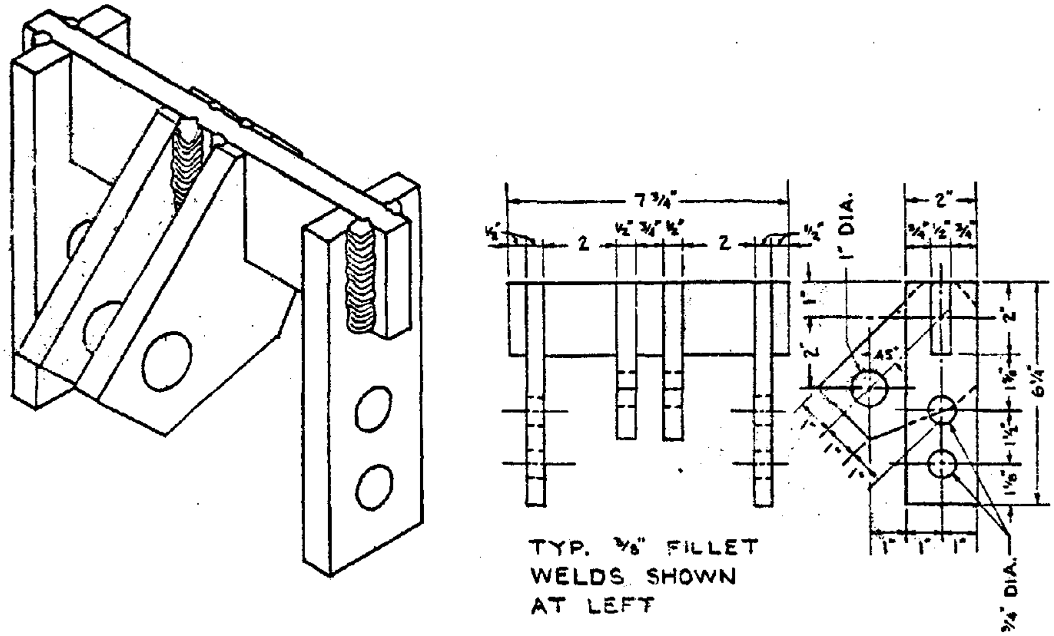

FIGURE 1 TYPE A DEVICE

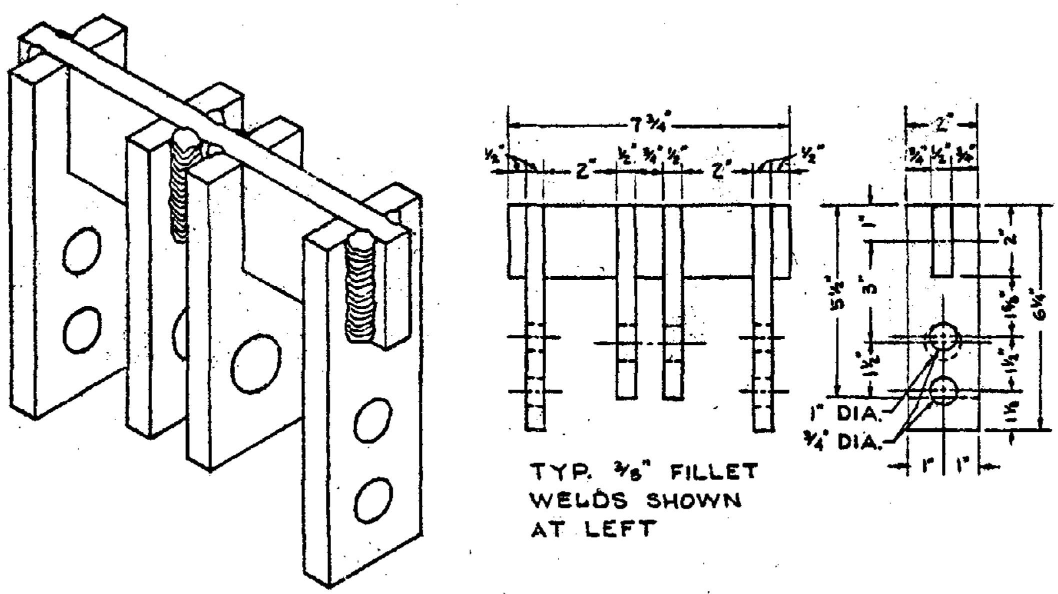

FIGURE 2 TYPE B DEVICE

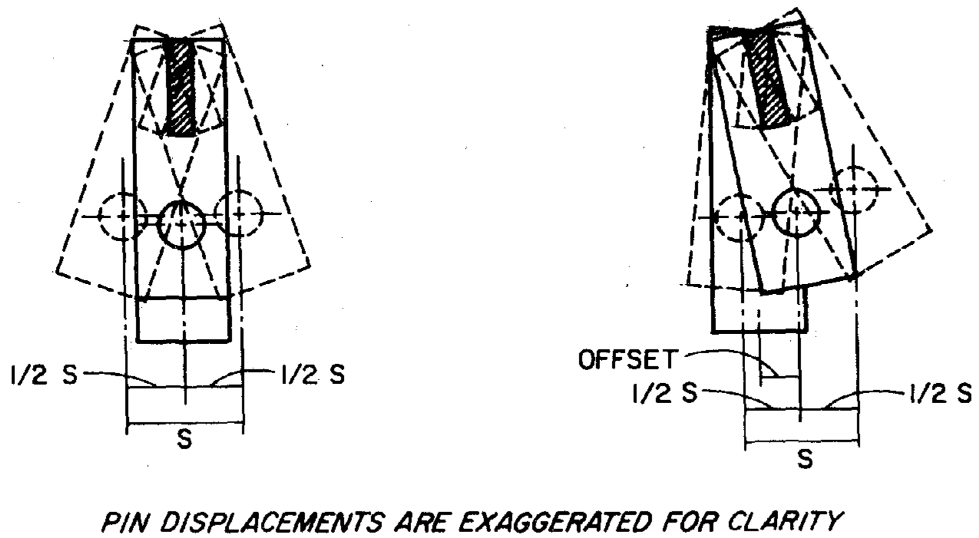

FIGURE 3 SYMMETRIC AND ASYMMETRIC LOADING

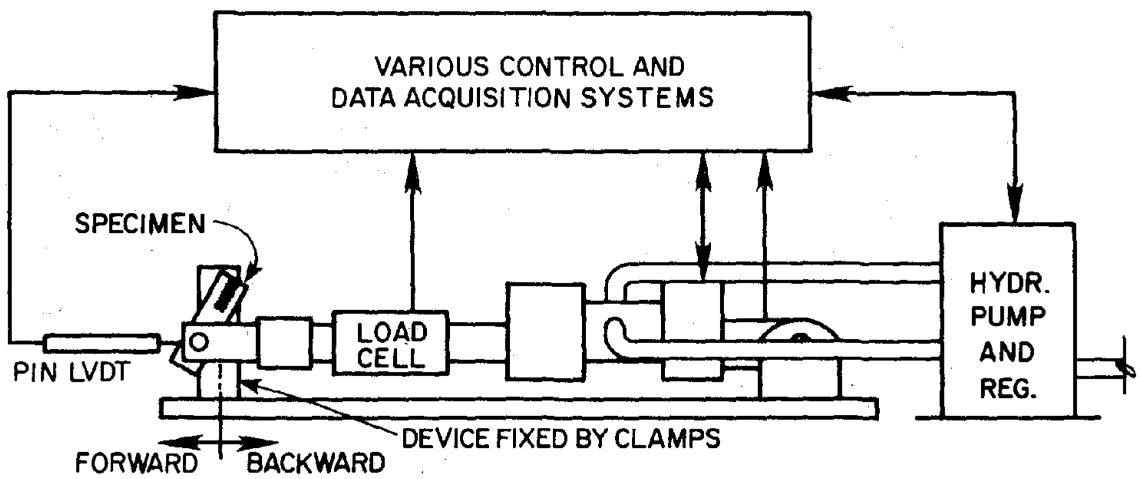

FIGURE 4 TORQUE APPLICATION

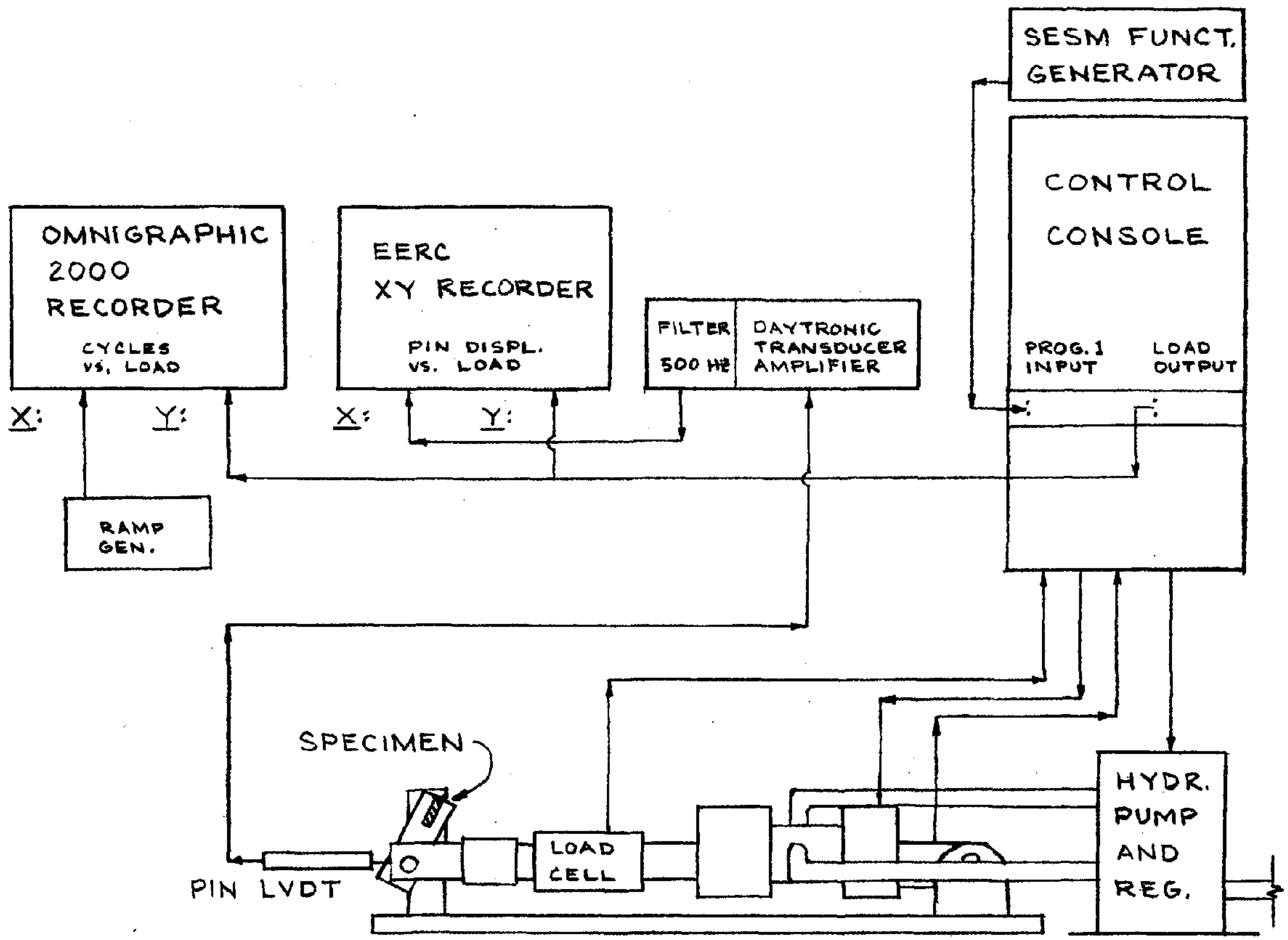

FIGURE 5 SETUP FOR INITIAL SINUSOIDAL LOADING TESTS

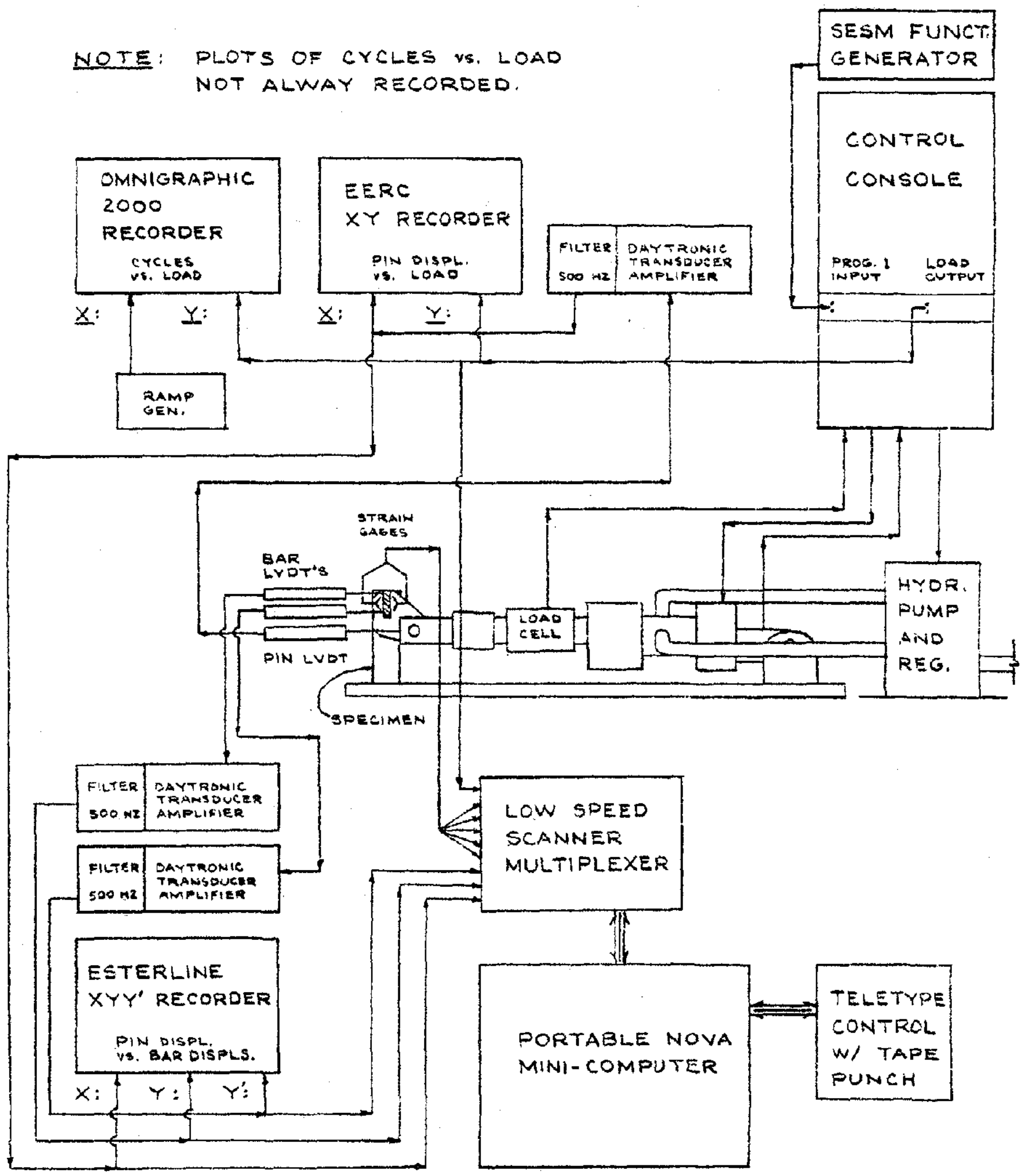

FIGURE 6 TESTING SETUP FOR SINUSOIDAL LOADING

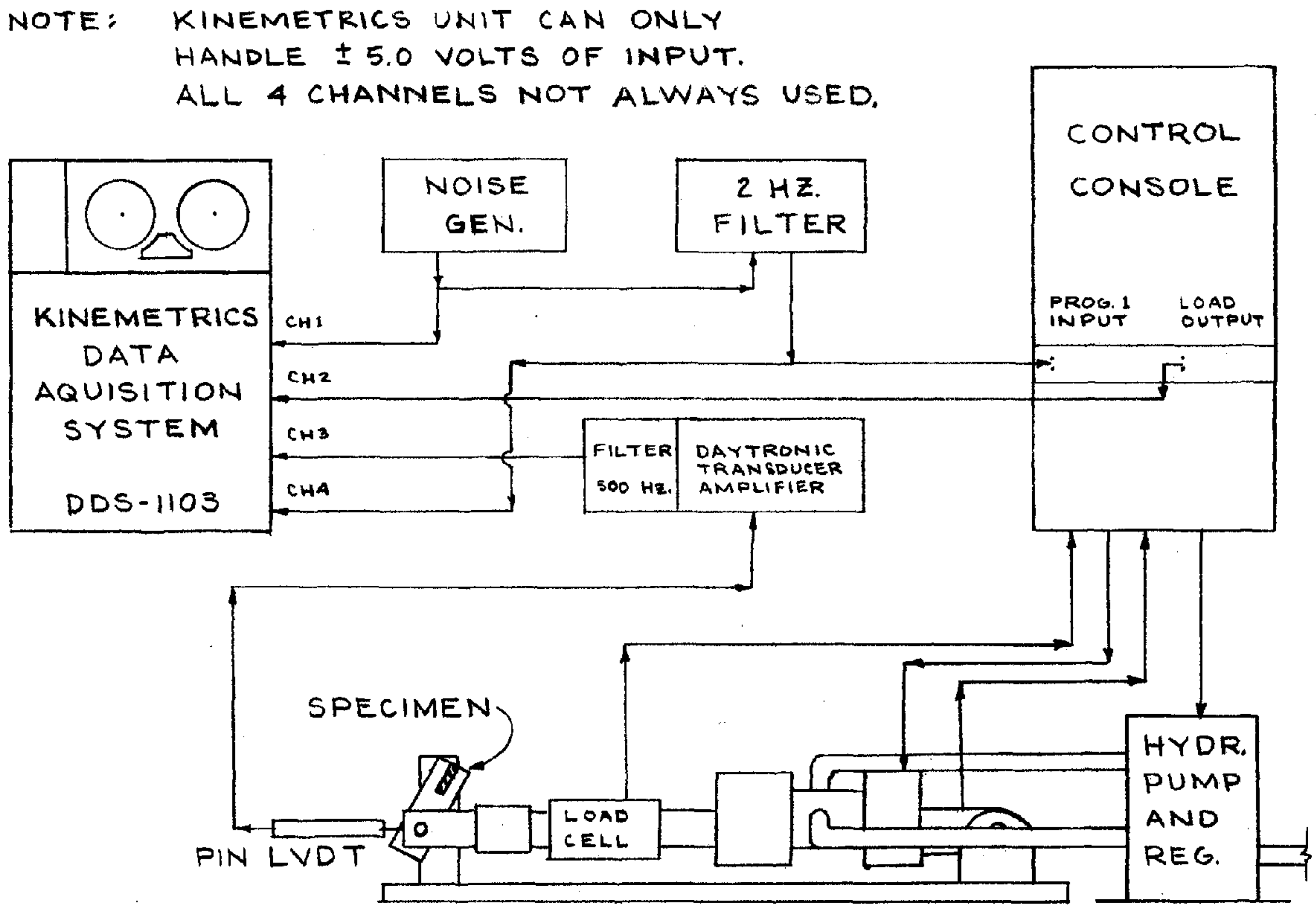

FIGURE 7 SETUP OF NOISE GENERATOR

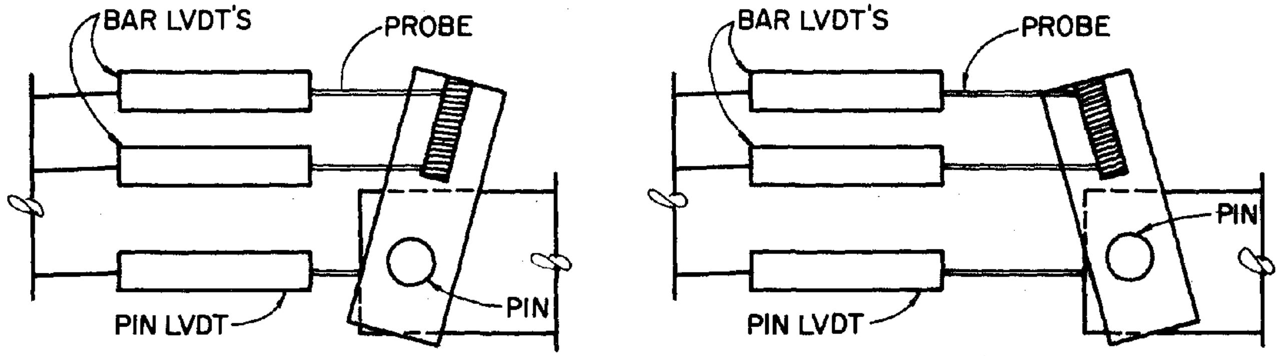

FIGURE 8 TORSION BAR AND PIN DISPLACEMENT MEASUREMENTS

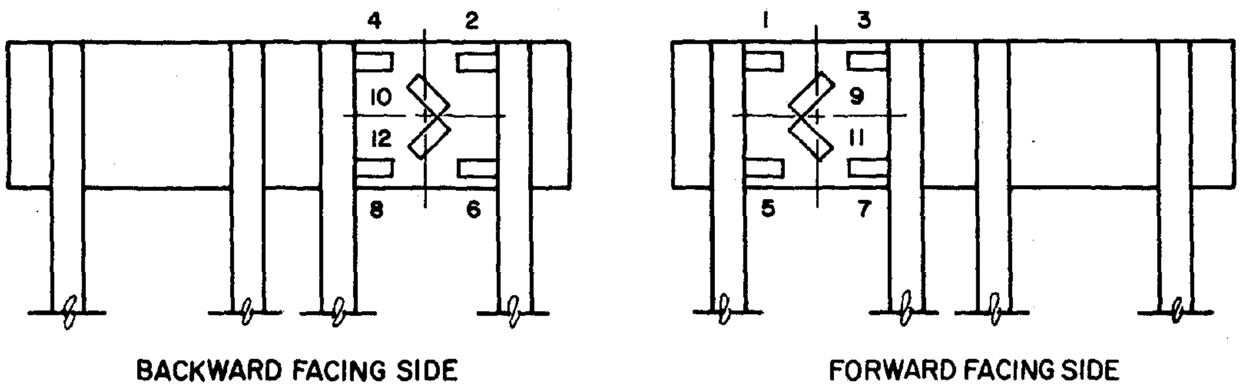

BENDING HALF BRIDGES: 1,2; 3,4; 5,6; 7,8
TORSION FULL BRIDGE: 9, 10, 11, 12

FIGURE 9 STRAIN GAGE DISTRIBUTION

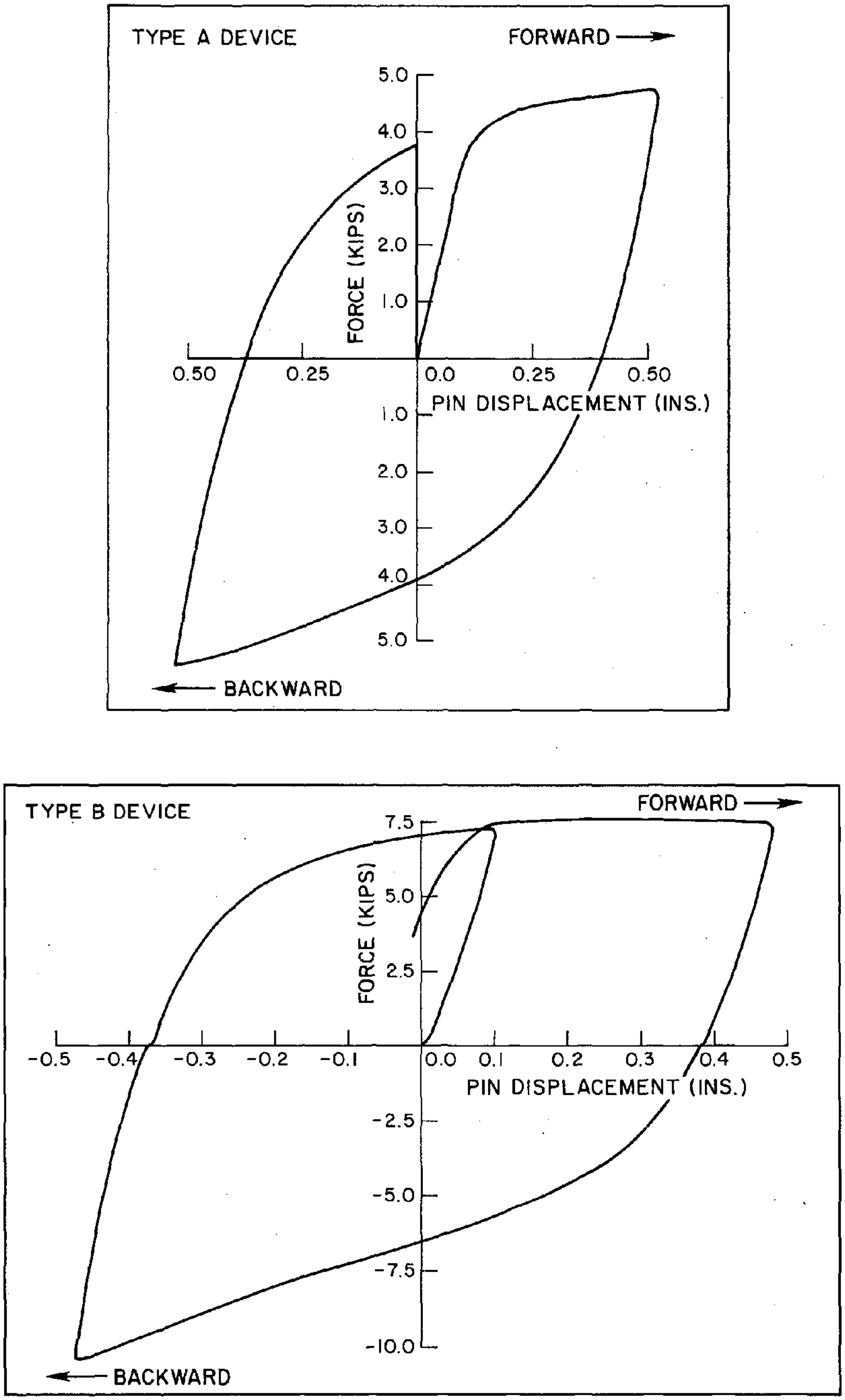

FIGURE 10 EFFECT OF CHANGES IN GEOMETRIC CONFIGURATION ON RESPONSE

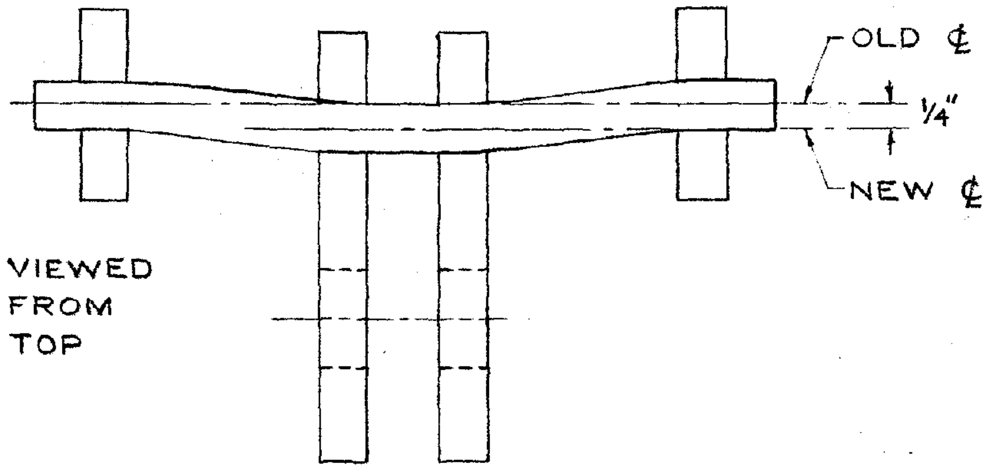

FIGURE 11 PERMANENT DEFORMATION OF TYPE B DEVICES AFTER 300 CYCLES OF SINUSOIDAL LOADING

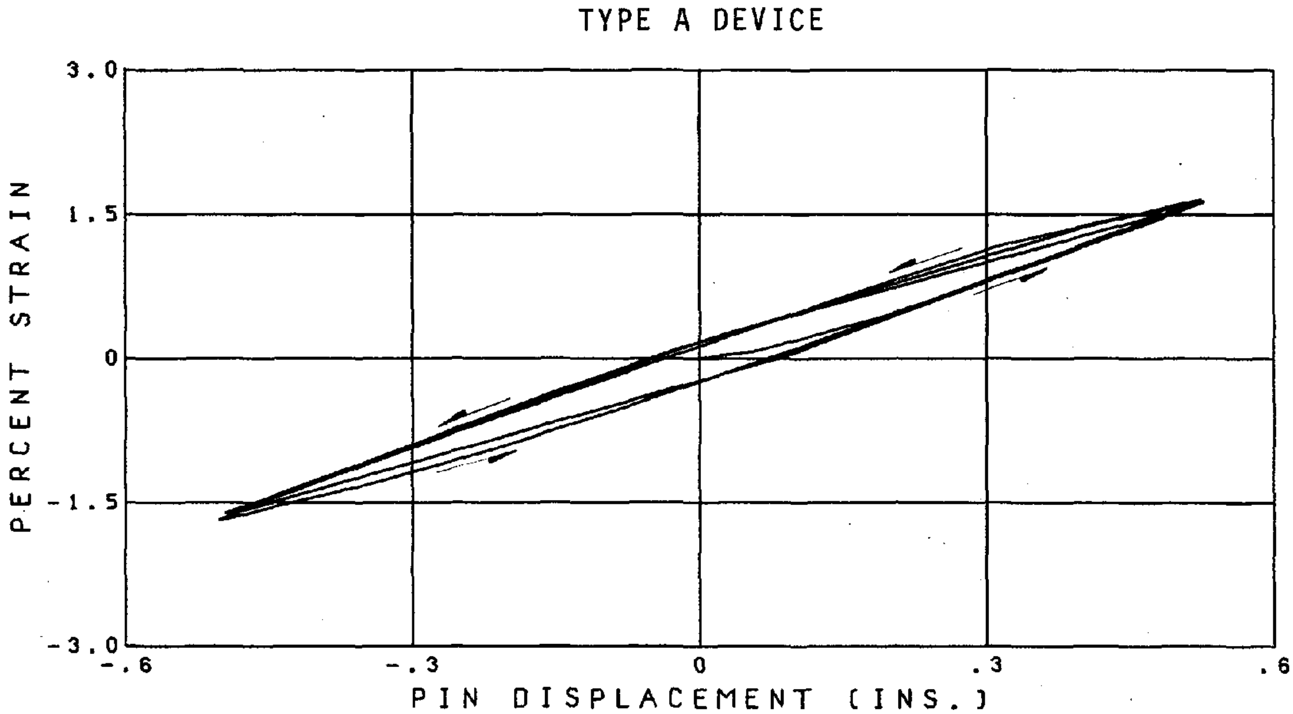

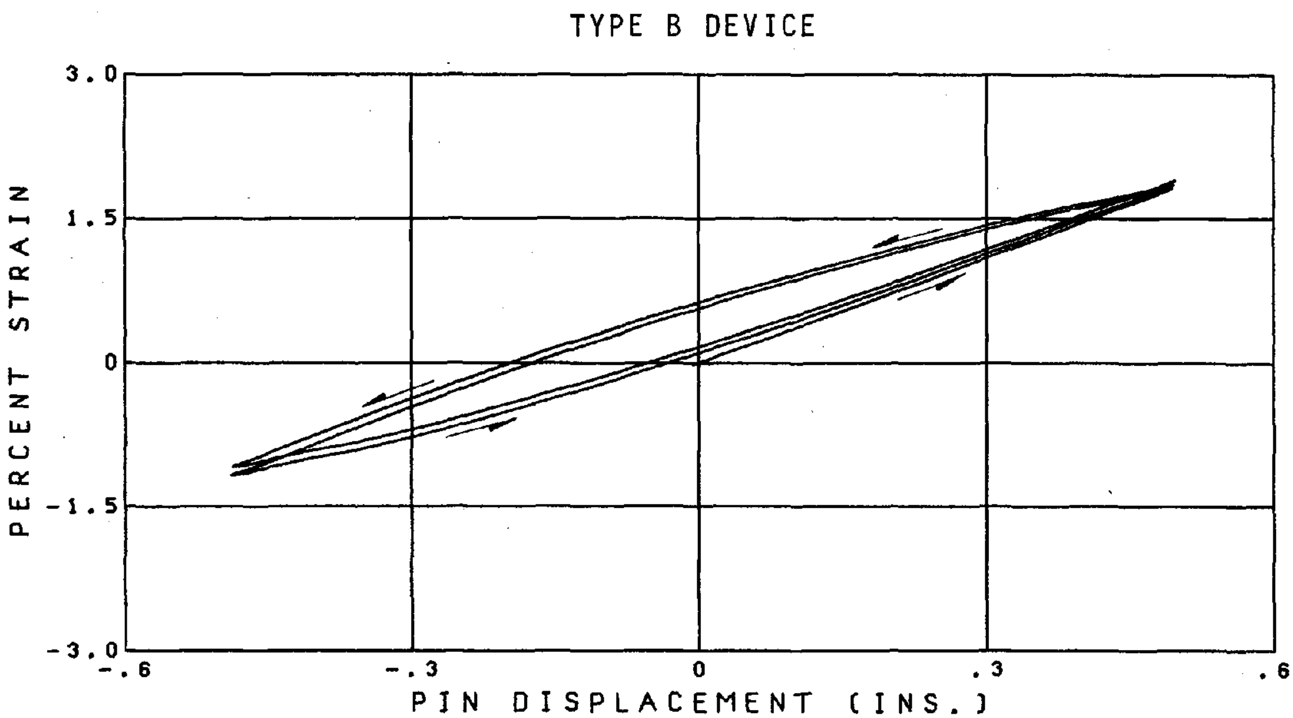

FIGURE 12 TORSIONAL STRAIN MEASURED AT MID-DEPTH OF TORSION BARS OF TYPES A AND B DEVICE

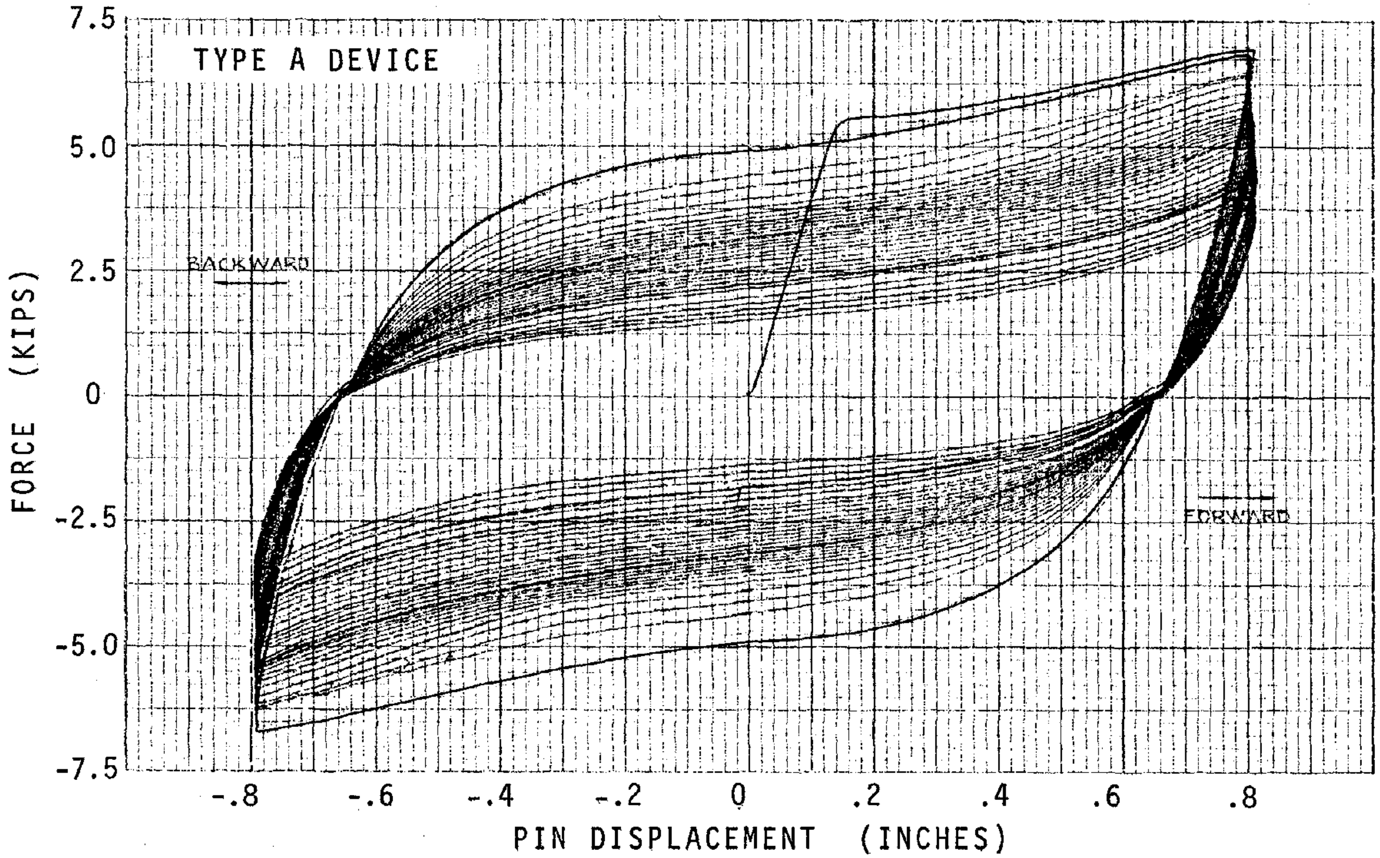

FIGURE 13A HYSTERESIS OF TYPE A DEVICE UNDER SINUSOIDAL LOADING AFTER INITIAL STRAIN-HARDENING

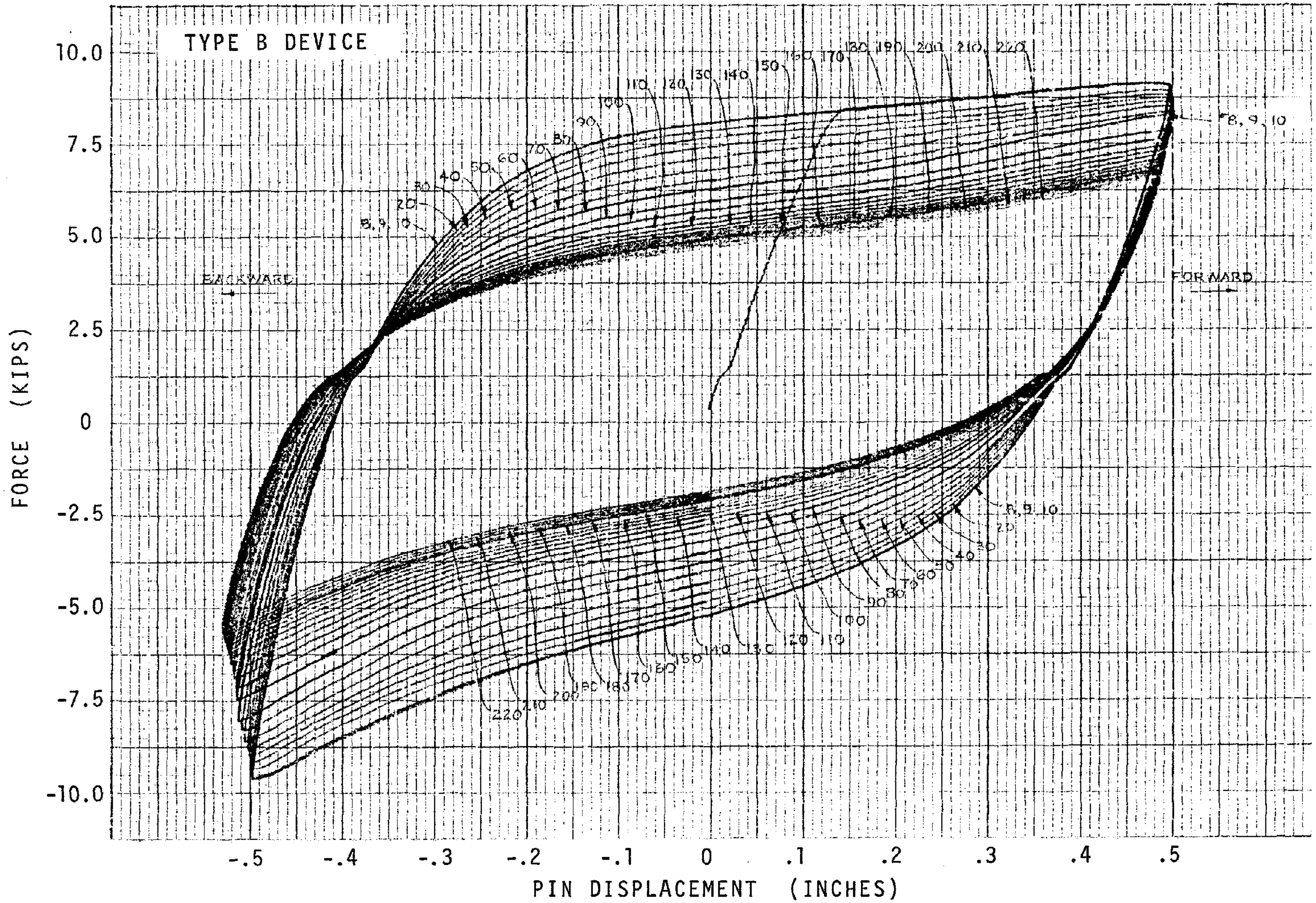

FIGURE 13B HYSTERESIS OF TYPE B DEVICE UNDER SINUSOIDAL LOADING AFTER INITIAL STRAIN-HARDENING

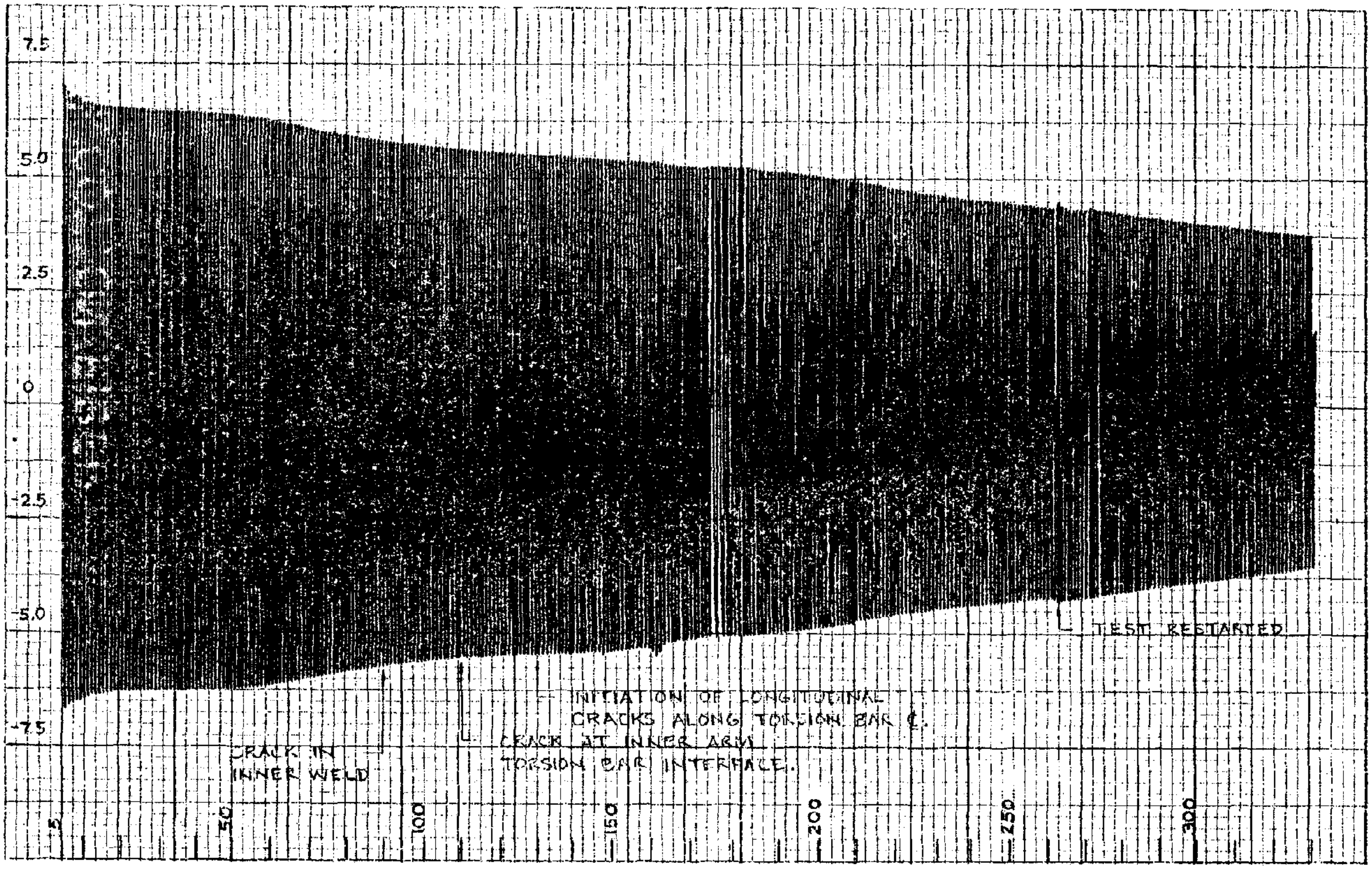

FIGURE 14A FORCE DECAY OF TYPE A DEVICE UNDER SINUSOIDAL LOADING AFTER INITIAL STRAIN-HARDENING

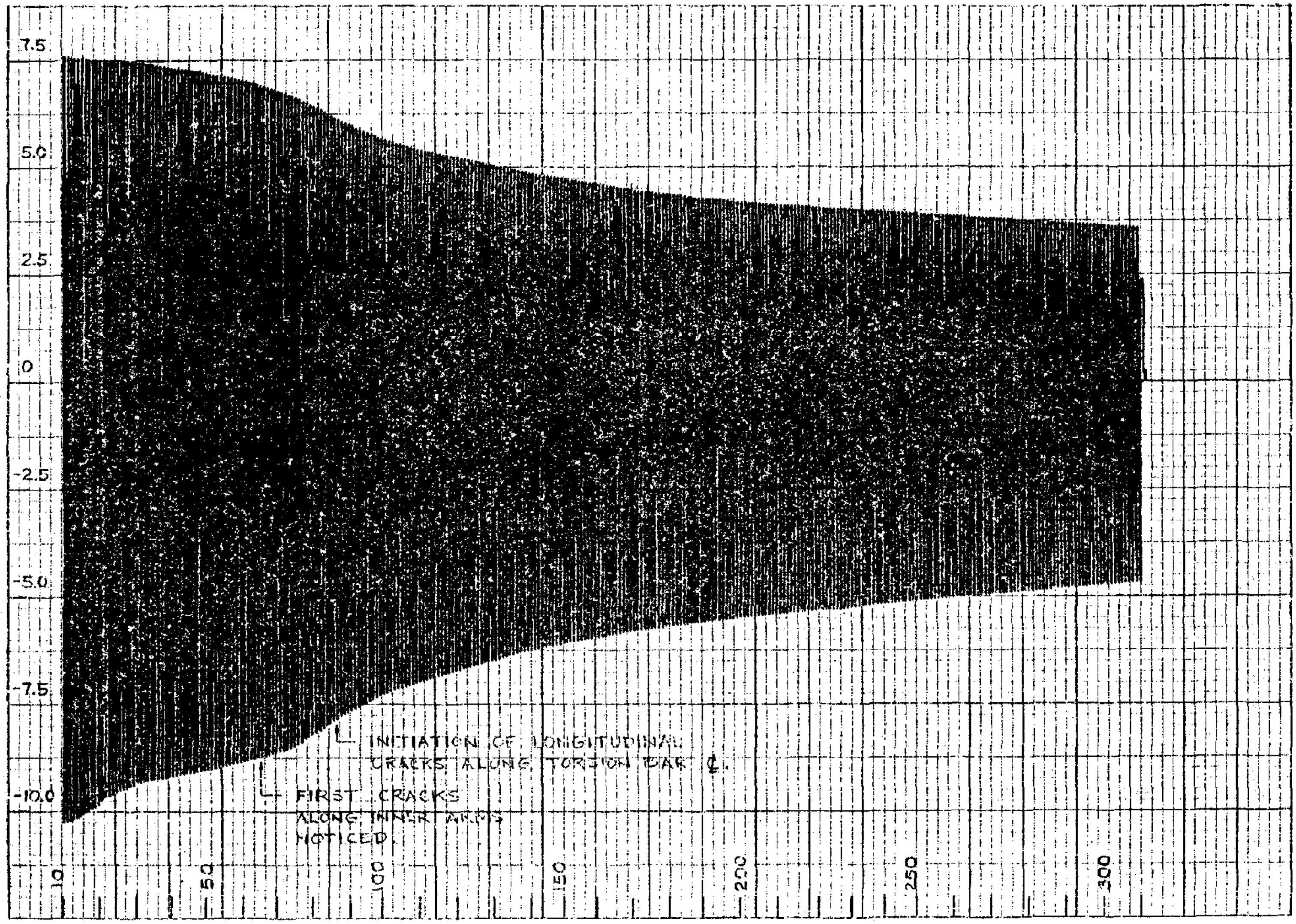

FIGURE 14B FORCE DECAY OF TYPE B DEVICE UNDER SINUSOIDAL LOADING AFTER INITIAL STRAIN-HARDENING

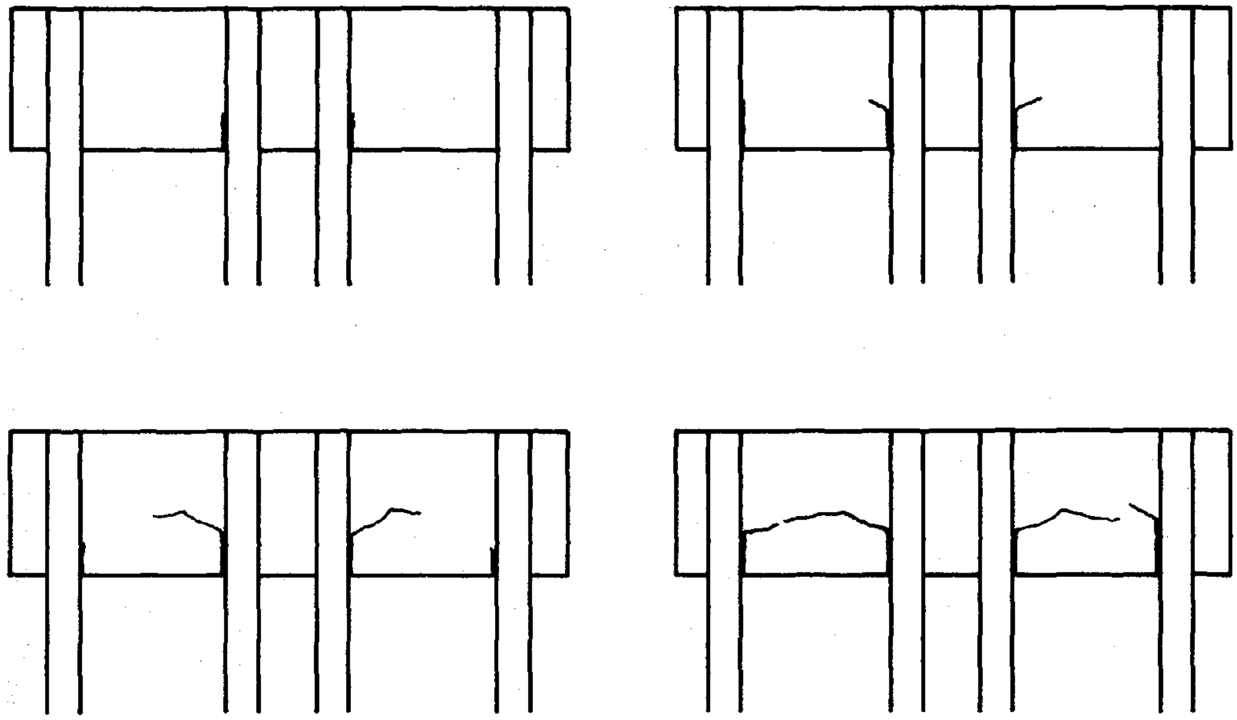

FIGURE 15 TYPICAL CRACK DEVELOPMENT ON FORWARD FACING SIDE OF TYPE B DEVICES SUBJECTED TO SINUSOIDAL LOADING

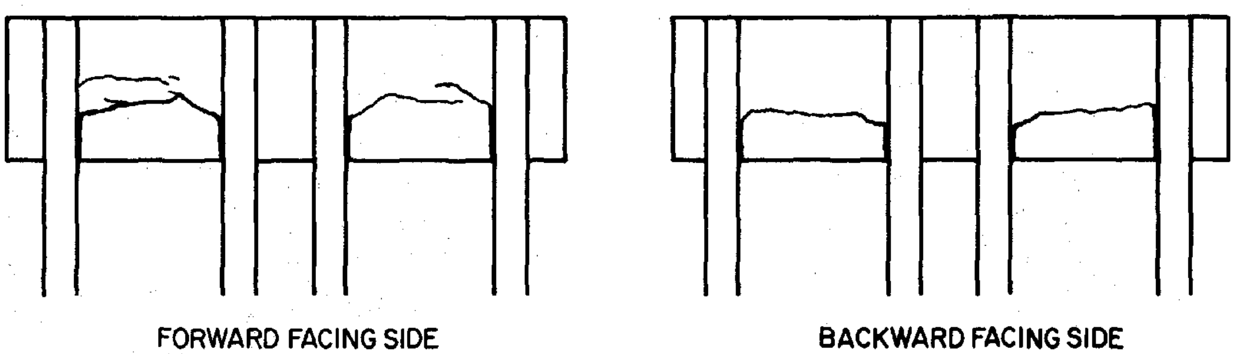

FIGURE 16 FINAL CRACKING PATTERN OF TYPE B DEVICES SUBJECTED TO SINUSOIDAL LOADING

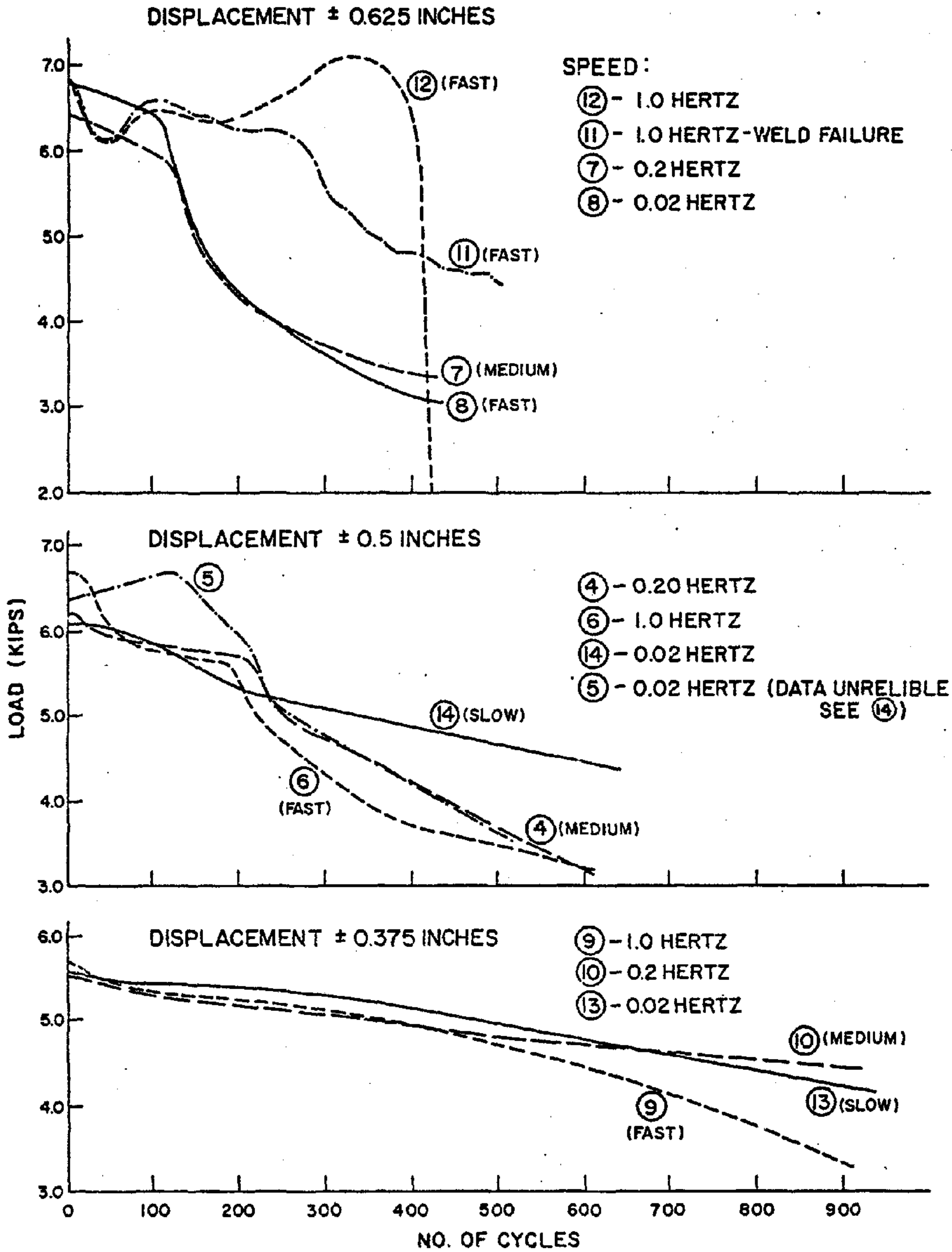

FIGURE 17 EFFECT OF LOADING RATE ON DEVICE RESPONSE

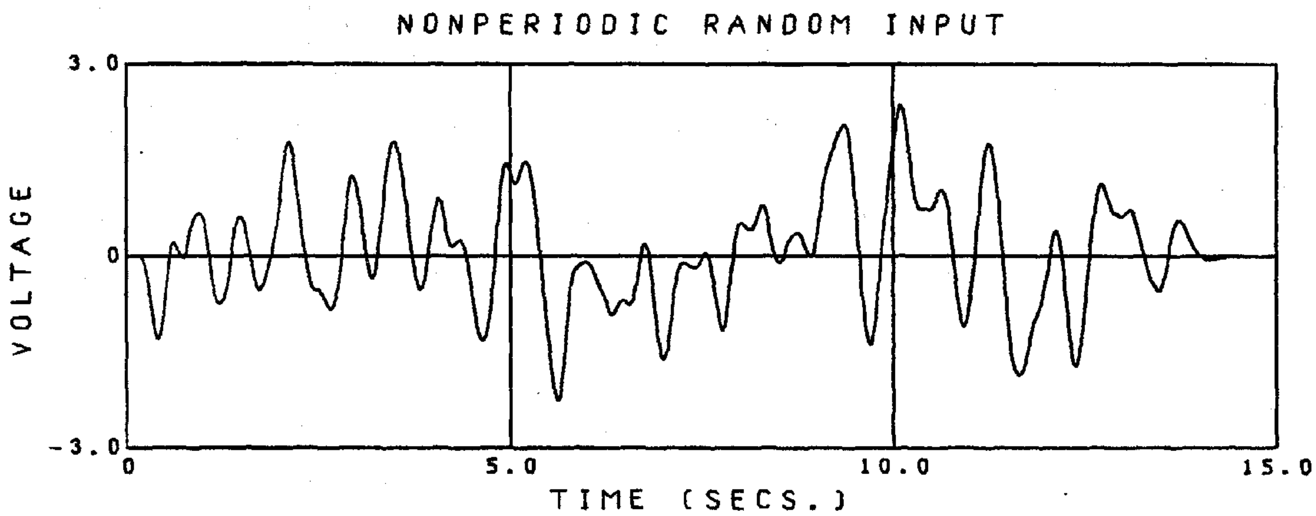

FIGURE 18 INITIAL 14.5 SECONDS OF NONPERIODIC FILTERED NOISE GENERATOR INPUT FUNCTION

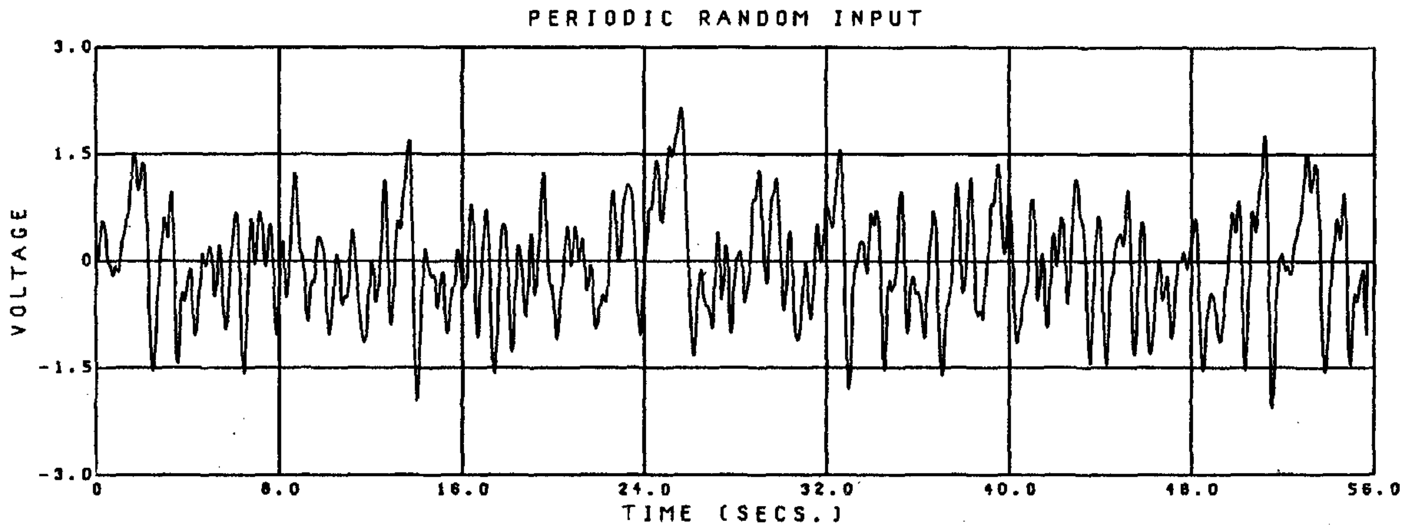

FIGURE 19 PERIODIC FILTERED NOISE GENERATOR INPUT FUNCTION - PERIOD OF 51.5 SECONDS

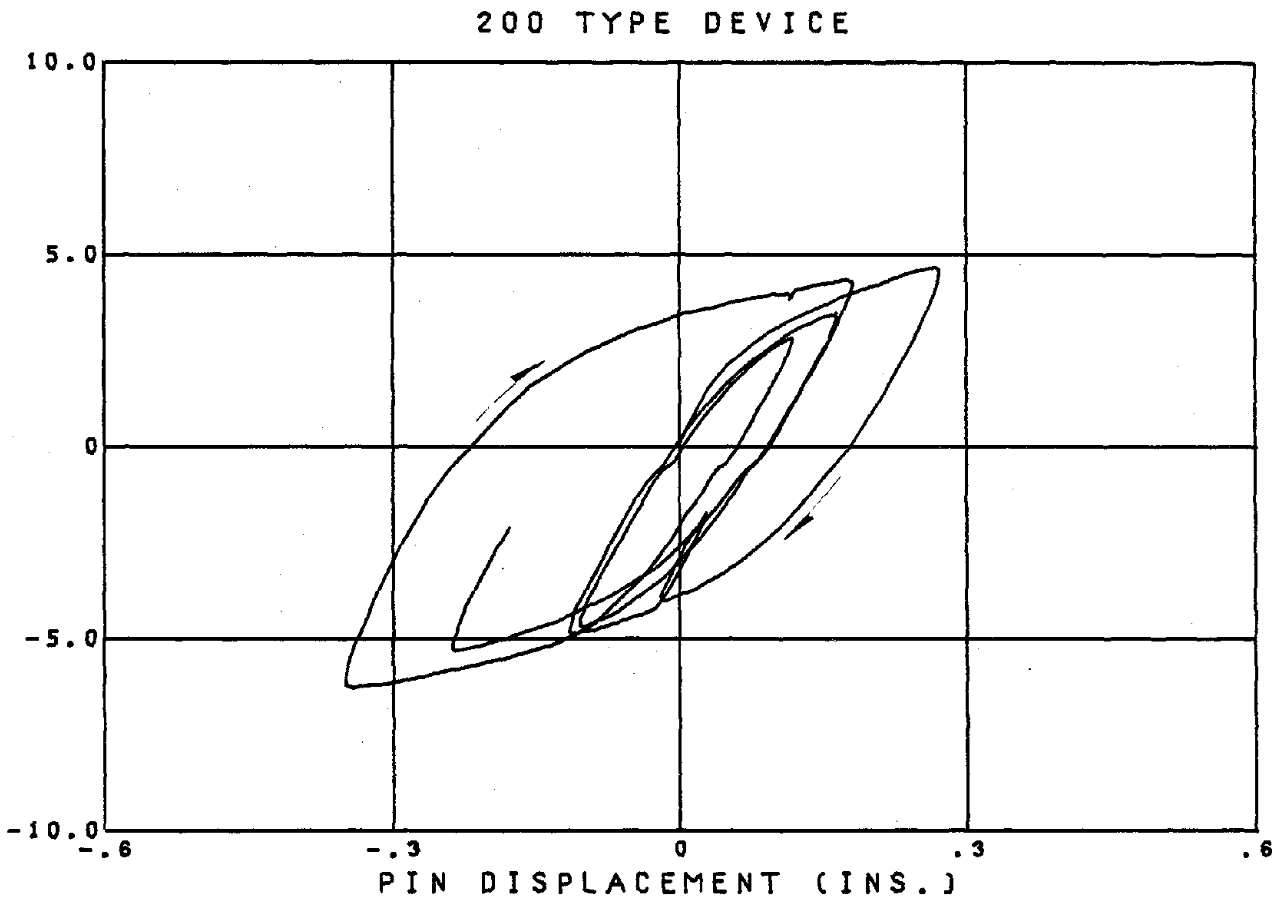

FIGURE 20 HYSTERESIS OF TYPE A DEVICES UNDER NONPERIODIC RANDOM LOADING

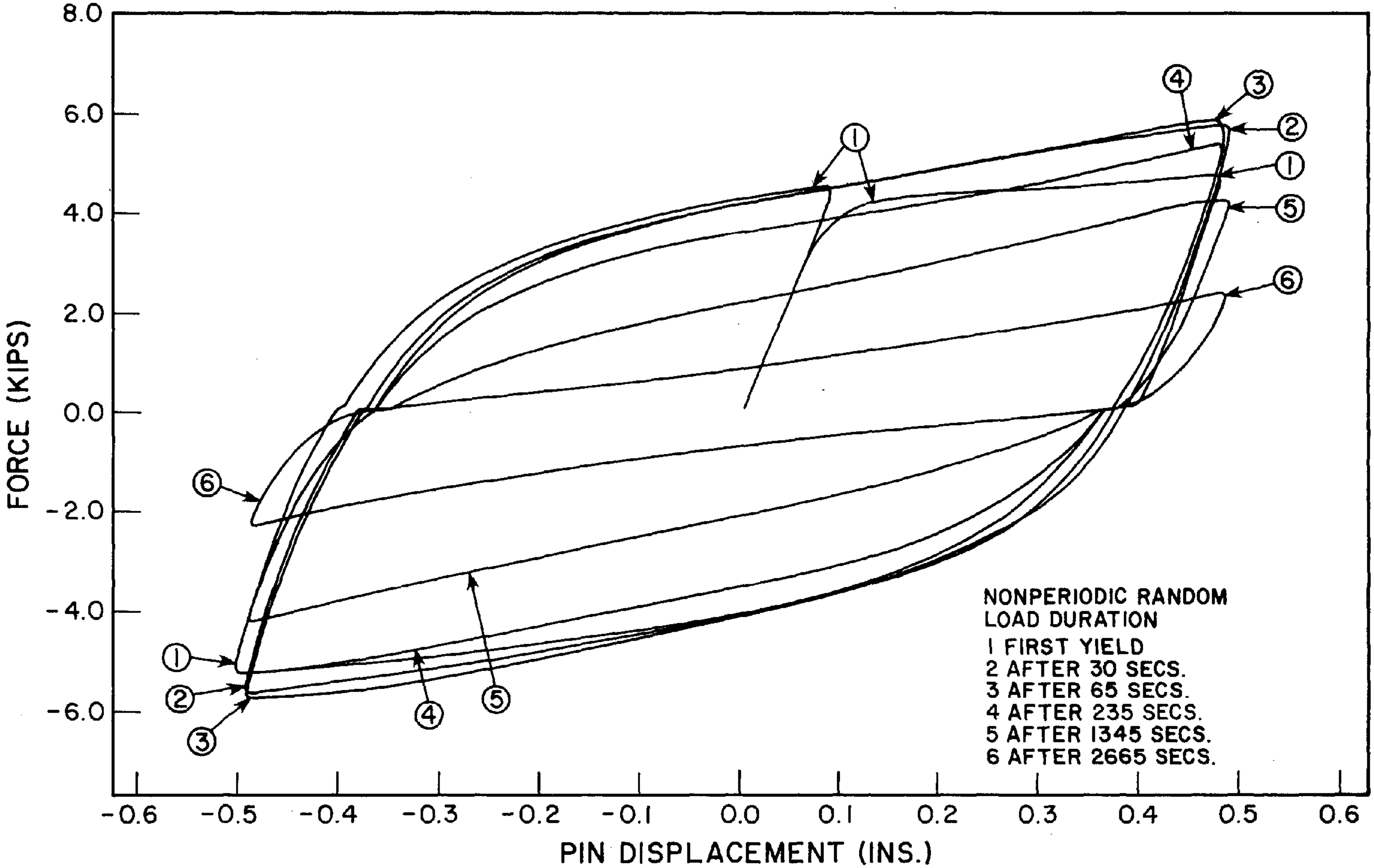

FIGURE 21 FORCE DECAY OF TYPE A DEVICES UNDER NONPERIODIC RANDOM LOADING AS MONITORED BY INTERMITTENT SINUSOIDAL HYSTERESIS LOOPS

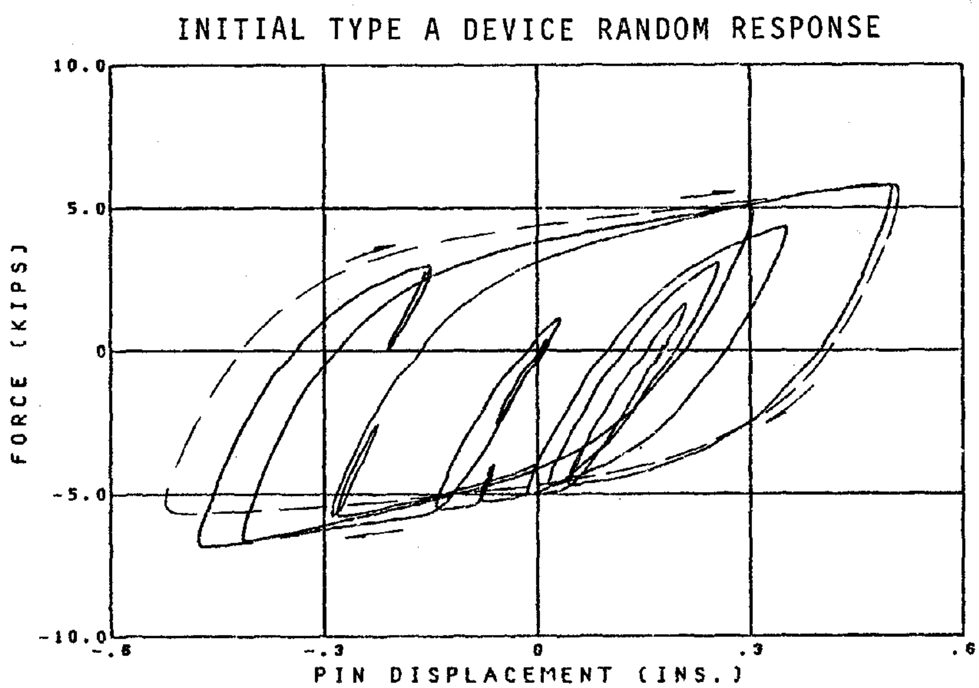

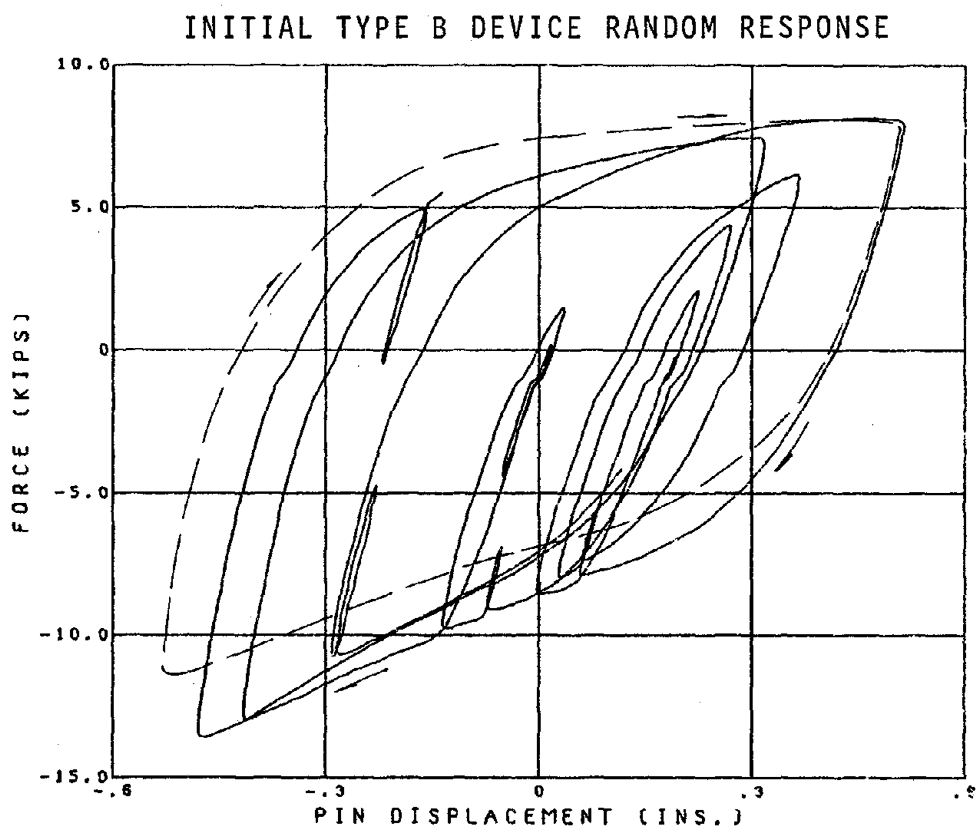

FIGURE 22 HYSTERESIS OF TYPES A AND B DEVICE UNDER NONPERIODIC RANDOM LOADING - FIVE-SECOND RESPONSE & CORRESPONDING SINUSOIDAL BOUND SHOWN FOR EACH

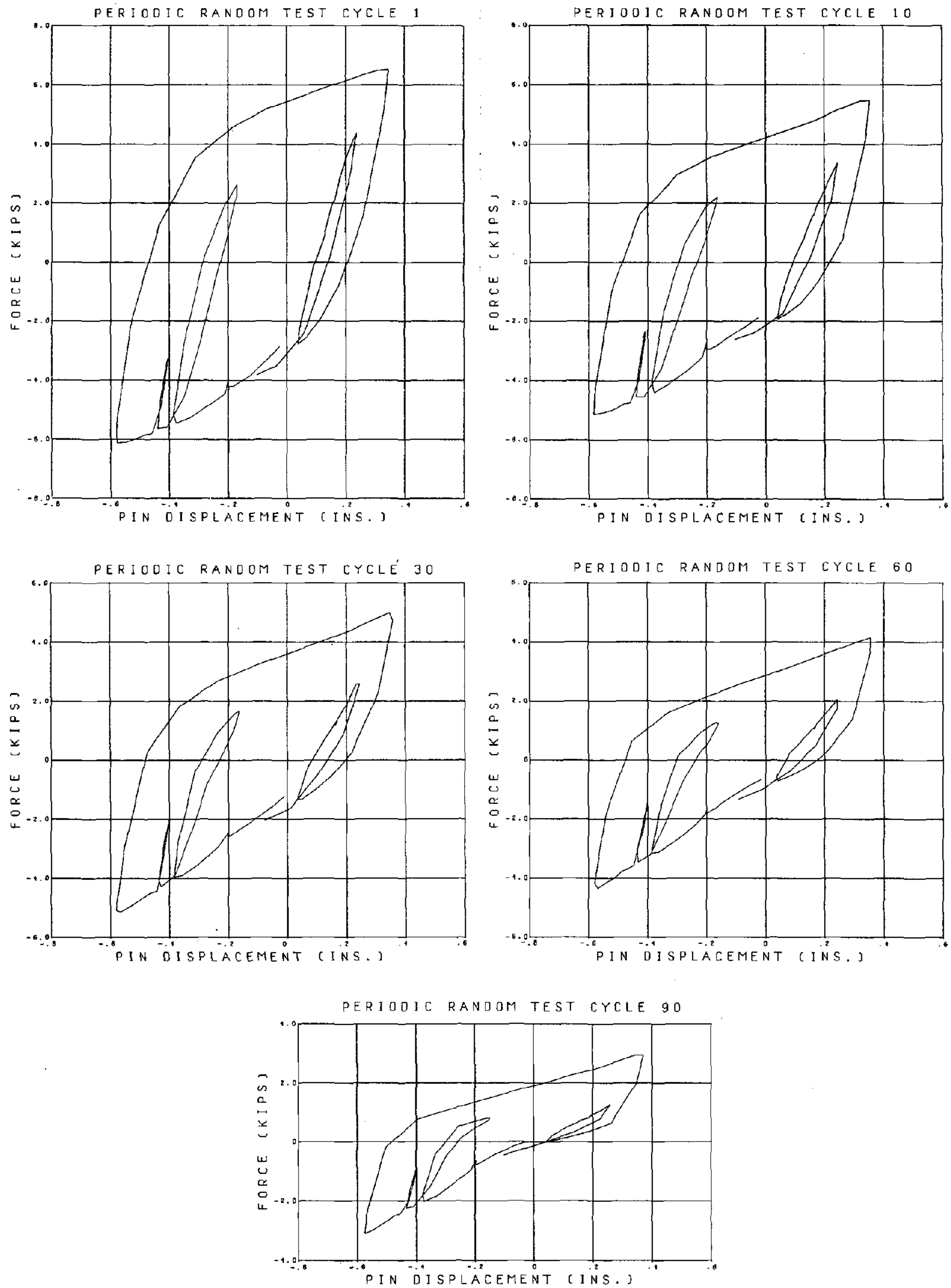

FIGURE 23 HYSTERESIS OF TYPE A DEVICE THROUGH 90 PERIODS OF PERIODIC RANDOM LOADING - 3.2 SECONDS OF RESPONSE TAKEN 24 SECONDS AFTER THE CYCLE BEGAN

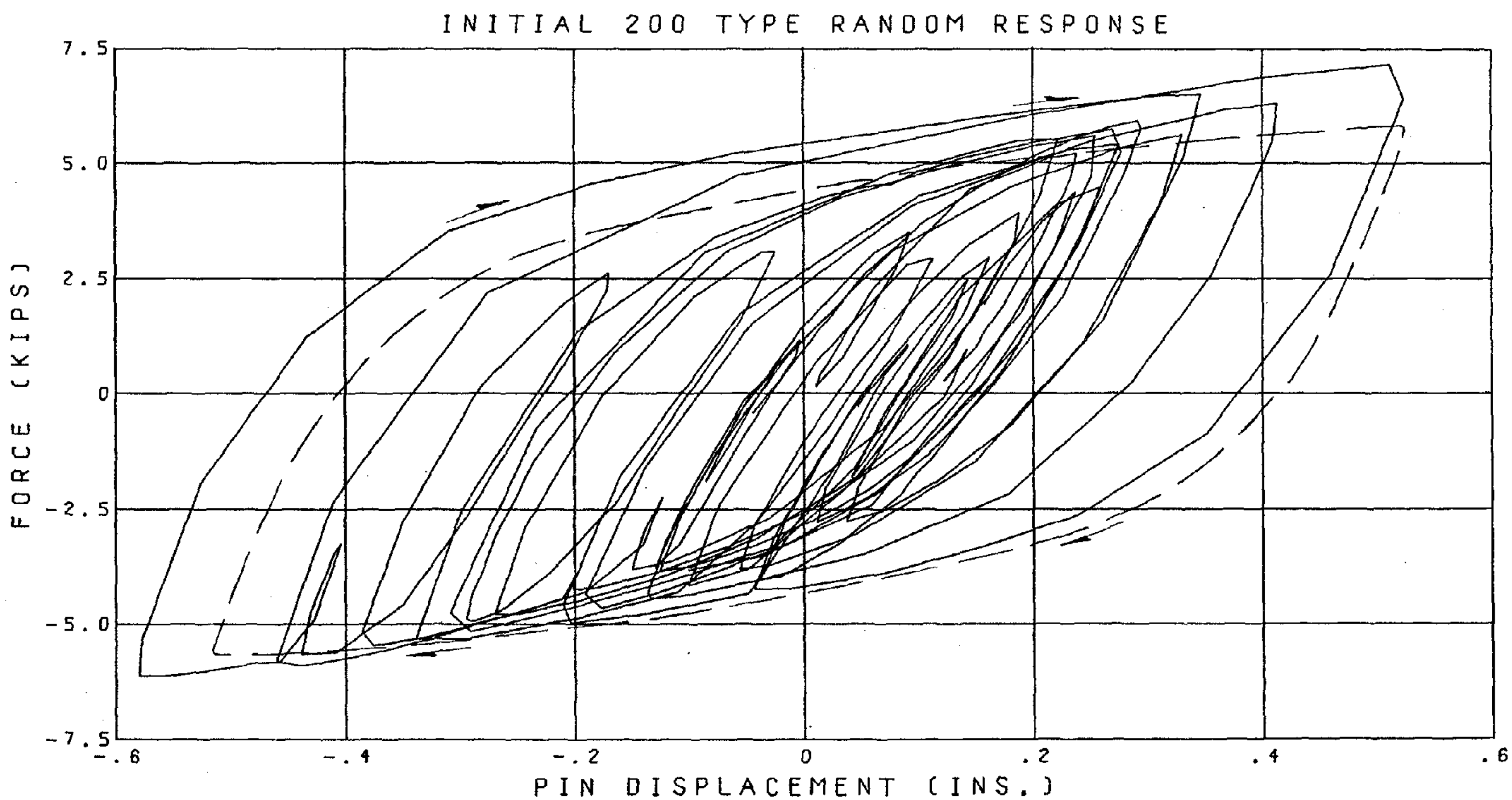

FIGURE 24 COMPARISON OF PERIODIC RANDOM AND SINUSOIDAL HYSTERESIS FOR A TYPE A DEVICE - ±1/2 IN. (±1.27 CM.) NOMINAL STROKE

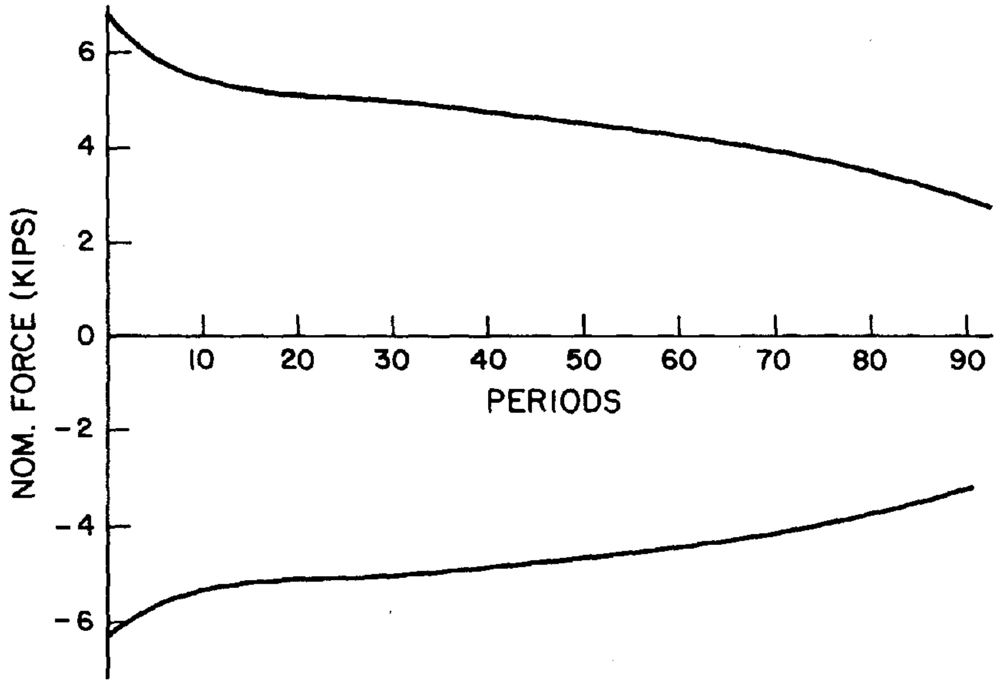

FIGURE 25 NOMINAL FORCE DECAY OF A TYPE A DEVICE UNDER PERIODIC RANDOM LOADING

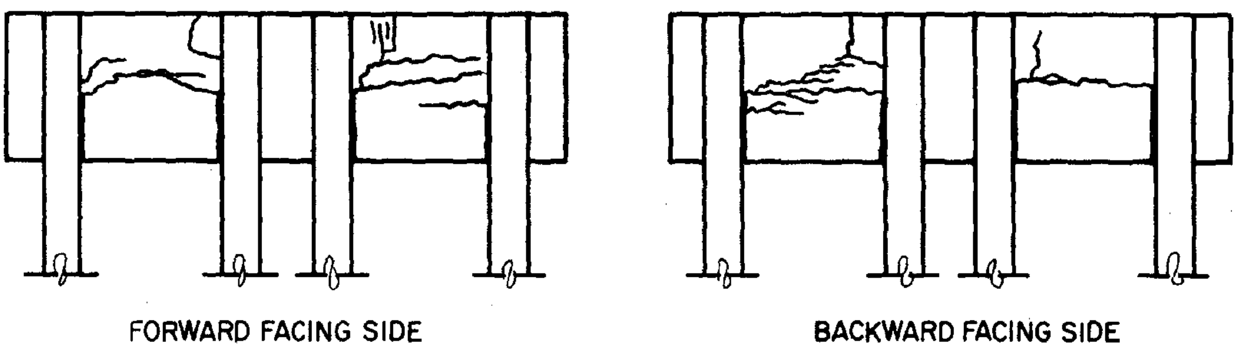

FIGURE 26 FINAL CRACKING PATTERN OF A TYPE A DEVICE SUBJECTED TO PERIODIC RANDOM LOADING

EARTHQUAKE ENGINEERING RESEARCH CENTER REPORTS

EARTHQUAKE ENGINEERING RESEARCH CENTER REPORTS

NOTE: Numbers in parenthesis are Accession Numbers assigned by the National Technical Information Service; these are followed by a price code. Copies of the reports may be ordered from the National Technical Information Service, 5285 Port Royal Road, Springfield, Virginia, 22161. Accession Numbers should be quoted on orders for reports (PB --- ---) and remittance must accompany each order. Reports without this information were not available at time of printing. Upon request, EERC will mail inquirers this information when it becomes available.

EERC 67-1 "Feasibility Study Large-Scale Earthquake Simulator Facility," by J. Penzien, J.G. Bouwkamp, R.W. Clough and D. Rea - 1967 (PB 187 905)A07

EERC 68-1 Unassigned

EERC 68-2 "Inelastic Behavior of Beam-to-Column Subassemblages Under Repeated Loading," by V.V. Bertero - 1968 (PB 184 888)A05

EERC 68-3 "A Graphical Method for Solving the Wave Reflection-Refraction Problem," by H.D. McNiven and Y. Mengi - 1968 (PB 187 943)A03

EERC 68-4 "Dynamic Properties of McKinley School Buildings," by D. Rea, J.G. Bouwkamp and R.W. Clough - 1968 (PB 187 902)A07

EERC 68-5 "Characteristics of Rock Motions During Earthquakes," by H.B. Seed, I.M. Idriss and F.W. Kiefer - 1968 (PB 188 338)A03

EERC 69-1 "Earthquake Engineering Research at Berkeley," - 1969 (PB 187 906)A11

EERC 69-2 "Nonlinear Seismic Response of Earth Structures," by M. Dibaj and J. Penzien - 1969 (PB 187 904)A08

EERC 69-3 "Probabilistic Study of the Behavior of Structures During Earthquakes," by R. Ruiz and J. Penzien - 1969 (PB 187 886)A06

EERC 69-4 "Numerical Solution of Boundary Value Problems in Structural Mechanics by Reduction to an Initial Value Formulation," by N. Distefano and J. Schujman - 1969 (PB 187 942)A02

EERC 69-5 "Dynamic Programming and the Solution of the Biharmonic Equation," by N. Distefano - 1969 (PB 187 941)A03

EERC 69-6 "Stochastic Analysis of Offshore Tower Structures," by A.K. Malhotra and J. Penzien - 1969 (PB 187 903)A09

EERC 69-7 "Rock Motion Accelerograms for High Magnitude Earthquakes," by H.B. Seed and I.M. Idriss - 1969 (PB 187 940)A02

EERC 69-8 "Structural Dynamics Testing Facilities at the University of California, Berkeley," by R.M. Stephen, J.G. Bouwkamp, R.W. Clough and J. Penzien - 1969 (PB 189 111)A04

EERC 69-9 "Seismic Response of Soil Deposits Underlain by Sloping Rock Boundaries," by H. Dezfulian and H.B. Seed 1969 (PB 189 114)A03

EERC 69-10 "Dynamic Stress Analysis of Axisymmetric Structures Under Arbitrary Loading," by S. Ghosh and E.L. Wilson 1969 (PB 189 026)A10

EERC 69-11 "Seismic Behavior of Multistory Frames Designed by Different Philosophies," by J.C. Anderson and V. V. Bertero - 1969 (PB 190 662)A10

EERC 69-12 "Stiffness Degradation of Reinforcing Concrete Members Subjected to Cyclic Flexural Moments," by V.V. Bertero, B. Bresler and H. Ming Liao - 1969 (PB 202 942)A07

EERC 69-13 "Response of Non-Uniform Soil Deposits to Travelling Seismic Waves," by H. Dezfulian and H.B. Seed - 1969 (PB 191 023)A03

EERC 69-14 "Damping Capacity of a Model Steel Structure," by D. Rea, R.W. Clough and J.G. Bouwkamp - 1969 (PB 190 663)A06

EERC 69-15 "Influence of Local Soil Conditions on Building Damage Potential during Earthquakes," by H.B. Seed and I.M. Idriss - 1969 (PB 191 036)A03

EERC 69-16 "The Behavior of Sands Under Seismic Loading Conditions," by M.L. Silver and H.B. Seed - 1969 (AD 714 982)A07

EERC 70-1 "Earthquake Response of Gravity Dams," by A.K. Chopra - 1970 (AD 709 640)A03

EERC 70-2 "Relationships between Soil Conditions and Building Damage in the Caracas Earthquake of July 29, 1967," by H.B. Seed, I.M. Idriss and H. Dezfulian - 1970 (PB 195 762)A05

EERC 70-3 "Cyclic Loading of Full Size Steel Connections," by E.P. Popov and R.M. Stephen - 1970 (PB 213 545)A04

EERC 70-4 "Seismic Analysis of the Charaima Building, Caraballeda, Venezuela," by Subcommittee of the SEAONC Research Committee: V.V. Bertero, P.F. Fratessa, S.A. Mahin, J.H. Sexton, A.C. Scordelis, E.L. Wilson, L.A. Wyllie, H.B. Seed and J. Penzien, Chairman - 1970 (PB 201 455)A06

EERC 70-5 "A Computer Program for Earthquake Analysis of Dams," by A.K. Chopra and P. Chakrabarti - 1970 (AD 723 994)A05

EERC 70-6 "The Propagation of Love Waves Across Non-Horizontally Layered Structures," by J. Lysmer and L.A. Drake 1970 (PB 197 896)A03

EERC 70-7 "Influence of Base Rock Characteristics on Ground Response," by J. Lysmer, H.B. Seed and P.B. Schnabel 1970 (PB 197 897)A03

EERC 70-8 "Applicability of Laboratory Test Procedures for Measuring Soil Liquefaction Characteristics under Cyclic Loading," by H.B. Seed and W.H. Peacock - 1970 (PB 198 016)A03

EERC 70-9 "A Simplified Procedure for Evaluating Soil Liquefaction Potential," by H.B. Seed and I.M. Idriss - 1970 (PB 198 009)A03

EERC 70-10 "Soil Moduli and Damping Factors for Dynamic Response Analysis," by H.B. Seed and I.M. Idriss - 1970 (PB 197 869)A03

EERC 71-1 "Koyna Earthquake of December 11, 1967 and the Performance of Koyna Dam," by A.K. Chopra and P. Chakrabarti 1971 (AD 731 496)A06

EERC 71-2 "Preliminary In-Situ Measurements of Anelastic Absorption in Soils Using a Prototype Earthquake Simulator," by R.D. Borcherdt and P.W. Rodgers - 1971 (PB 201 454)A03

EERC 71-3 "Static and Dynamic Analysis of Inelastic Frame Structures," by F.L. Porter and G.H. Powell - 1971 (PB 210 135)A06

EERC 71-4 "Research Needs in Limit Design of Reinforced Concrete Structures," by V.V. Bertero - 1971 (PB 202 943)A04

EERC 71-5 "Dynamic Behavior of a High-Rise Diagonally Braced Steel Building," by D. Rea, A.A. Shah and J.G. Bouwkamp 1971 (PB 203 584)A06

EERC 71-6 "Dynamic Stress Analysis of Porous Elastic Solids Saturated with Compressible Fluids," by J. Ghaboussi and E. L. Wilson - 1971 (PB 211 396)A06

EERC 71-7 "Inelastic Behavior of Steel Beam-to-Column Subassemblages," by H. Krawinkler, V.V. Bertero and E.P. Popov 1971 (PB 211 335)A14

EERC 71-8 "Modification of Seismograph Records for Effects of Local Soil Conditions," by P. Schnabel, H.B. Seed and J. Lysmer - 1971 (PB 214 450)A03

EERC 72-1 "Static and Earthquake Analysis of Three Dimensional Frame and Shear Wall Buildings," by E.L. Wilson and H.H. Dovey - 1972 (PB 212 904)A05

EERC 72-2 "Accelerations in Rock for Earthquakes in the Western United States," by P.B. Schnabel and H.B. Seed - 1972 (PB 213 100)A03

EERC 72-3 "Elastic-Plastic Earthquake Response of Soil-Building Systems," by T. Minami - 1972 (PB 214 868)A08

EERC 72-4 "Stochastic Inelastic Response of Offshore Towers to Strong Motion Earthquakes," by M.K. Kaul - 1972 (PB 215 713)A05

EERC 72-5 "Cyclic Behavior of Three Reinforced Concrete Flexural Members with High Shear," by E.P. Popov, V.V. Bertero and H. Krawinkler - 1972 (PB 214 555)A05

EERC 72-6 "Earthquake Response of Gravity Dams Including Reservoir Interaction Effects," by P. Chakrabarti and A.K. Chopra - 1972 (AD 762 330)A08

EERC 72-7 "Dynamic Properties of Pine Flat Dam," by D. Rea, C.Y. Liaw and A.K. Chopra - 1972 (AD 763 928)A05

EERC 72-8 "Three Dimensional Analysis of Building Systems," by E.L. Wilson and H.H. Dovey - 1972 (PB 222 438)A06

EERC 72-9 "Rate of Loading Effects on Uncracked and Repaired Reinforced Concrete Members," by S. Mahin, V.V. Bertero, D. Rea and M. Atalay - 1972 (PB 224 520)A08

EERC 72-10 "Computer Program for Static and Dynamic Analysis of Linear Structural Systems," by E.L. Wilson, K.-J. Bathe, J.E. Peterson and H.H.Dovey - 1972 (PB 220 437)A04

EERC 72-11 "Literature Survey - Seismic Effects on Highway Bridges," by T. Iwasaki, J. Penzien and R.W. Clough - 1972 (PB 215 613)A19

EERC 72-12 "SHAKE-A Computer Program for Earthquake Response Analysis of Horizontally Layered Sites," by P.B. Schnabel and J. Lysmer - 1972 (PB 220 207)A06

EERC 73-1 "Optimal Seismic Design of Multistory Frames," by V.V. Bertero and H. Kamil - 1973

EERC 73-2 "Analysis of the Slides in the San Fernando Dams During the Earthquake of February 9, 1971," by H.B. Seed, K.L. Lee, I.M. Idriss and F. Makdisi - 1973 (PB 223 402)A14

EERC 73-3 "Computer Aided Ultimate Load Design of Unbraced Multistory Steel Frames," by M.B. El-Hafez and G.H. Powell 1973 (PB 248 315)A09

EERC 73-4 "Experimental Investigation into the Seismic Behavior of Critical Regions of Reinforced Concrete Components as Influenced by Moment and Shear," by M. Celebi and J. Penzien - 1973 (PB 215 884)A09

EERC 73-5 "Hysteretic Behavior of Epoxy-Repaired Reinforced Concrete Beams," by M. Celebi and J. Penzien - 1973 (PB 239 568)A03

EERC 73-6 "General Purpose Computer Program for Inelastic Dynamic Response of Plane Structures," by A. Kanaan and G.H. Powell - 1973 (PB 221 260)A08

EERC 73-7 "A Computer Program for Earthquake Analysis of Gravity Dams Including Reservoir Interaction," by P. Chakrabarti and A.K. Chopra - 1973 (AD 766 271)A04

EERC 73-8 "Behavior of Reinforced Concrete Deep Beam-Column Subassemblages Under Cyclic Loads," by O. Küstü and J.G. Bouwkamp - 1973 (PB 246 117)A12

EERC 73-9 "Earthquake Analysis of Structure-Foundation Systems," by A.K. Vaish and A.K. Chopra - 1973 (AD 766 272)A07

EERC 73-10 "Deconvolution of Seismic Response for Linear Systems," by R.B. Reimer - 1973 (PB 227 179)A08

EERC 73-11 "SAP IV: A Structural Analysis Program for Static and Dynamic Response of Linear Systems," by K.-J. Bathe, E.L. Wilson and F.E. Peterson - 1973 (PB 221 967)A09

EERC 73-12 "Analytical Investigations of the Seismic Response of Long, Multiple Span Highway Bridges," by W.S. Tseng and J. Penzien - 1973 (PB 227 816)A10

EERC 73-13 "Earthquake Analysis of Multi-Story Buildings Including Foundation Interaction," by A.K. Chopra and J.A. Gutierrez - 1973 (PB 222 970)A03

EERC 73-14 "ADAP: A Computer Program for Static and Dynamic Analysis of Arch Dams," by R.W. Clough, J.M. Raphael and S. Mojtahedi - 1973 (PB 223 763)A09

EERC 73-15 "Cyclic Plastic Analysis of Structural Steel Joints," by R.B. Pinkney and R.W. Clough - 1973 (PB 226 843)A08

EERC 73-16 "QUAD-4: A Computer Program for Evaluating the Seismic Response of Soil Structures by Variable Damping Finite Element Procedures," by I.M. Idriss, J. Lysmer, R. Hwang and H.B. Seed - 1973 (PB 229 424)A05

EERC 73-17 "Dynamic Behavior of a Multi-Story Pyramid Shaped Building," by R.M. Stephen, J.P. Hollings and J.G. Bouwkamp - 1973 (PB 240 718)A06

EERC 73-18 "Effect of Different Types of Reinforcing on Seismic Behavior of Short Concrete Columns," by V.V. Bertero, J. Hollings, O. Küstü, R.M. Stephen and J.G. Bouwkamp - 1973

EERC 73-19 "Olive View Medical Center Materials Studies, Phase I," by B. Bresler and V.V. Bertero - 1973 (PB 235 986)A06

EERC 73-20 "Linear and Nonlinear Seismic Analysis Computer Programs for Long Multiple-Span Highway Bridges," by W.S. Tseng and J. Penzien - 1973

EERC 73-21 "Constitutive Models for Cyclic Plastic Deformation of Engineering Materials," by J.M. Kelly and P.P. Gillis 1973 (PB 226 024)A03

EERC 73-22 "DRAIN - 2D User's Guide," by G.H. Powell - 1973 (PB 227 016)A05

EERC 73-23 "Earthquake Engineering at Berkeley - 1973," (PB 226 033)A11

EERC 73-24 Unassigned

EERC 73-25 "Earthquake Response of Axisymmetric Tower Structures Surrounded by Water," by C.Y. Liaw and A.K. Chopra 1973 (AD 773 052)A09

EERC 73-26 "Investigation of the Failures of the Olive View Stairtowers During the San Fernando Earthquake and Their Implications on Seismic Design," by V.V. Bertero and R.G. Collins - 1973 (PB 235 106)A13

EERC 73-27 "Further Studies on Seismic Behavior of Steel Beam-Column Subassemblages," by V.V. Bertero, H. Krawinkler and E.P. Popov - 1973 (PB 234 172)A06

EERC 74-1 "Seismic Risk Analysis," by C.S. Oliveira - 1974 (PB 235 920)A06

EERC 74-2 "Settlement and Liquefaction of Sands Under Multi-Directional Shaking," by R. Pyke, C.K. Chan and H.B. Seed 1974

EERC 74-3 "Optimum Design of Earthquake Resistant Shear Buildings," by D. Ray, K.S. Pister and A.K. Chopra - 1974 (PB 231 172)A06

EERC 74-4 "LUSH - A Computer Program for Complex Response Analysis of Soil-Structure Systems," by J. Lysmer, T. Udaka, H.B. Seed and R. Hwang - 1974 (PB 236 796)A05

EERC 74-5 "Sensitivity Analysis for Hysteretic Dynamic Systems: Applications to Earthquake Engineering," by D. Ray 1974 (PB 233 213)A06

EERC 74-6 "Soil Structure Interaction Analyses for Evaluating Seismic Response," by H.B. Seed, J. Lysmer and R. Hwang 1974 (PB 236 519)A04

EERC 74-7 Unassigned

EERC 74-8 "Shaking Table Tests of a Steel Frame - A Progress Report," by R.W. Clough and D. Tang - 1974 (PB 240 869)A03

EERC 74-9 "Hysteretic Behavior of Reinforced Concrete Flexural Members with Special Web Reinforcement," by V.V. Bertero, E.P. Popov and T.Y. Wang - 1974 (PB 236 797)A07

EERC 74-10 "Applications of Reliability-Based, Global Cost Optimization to Design of Earthquake Resistant Structures," by E. Vitiello and K.S. Pister - 1974 (PB 237 231)A06

EERC 74-11 "Liquefaction of Gravelly Soils Under Cyclic Loading Conditions," by R.T. Wong, H.B. Seed and C.K. Chan 1974 (PB 242 042)A03

EERC 74-12 "Site-Dependent Spectra for Earthquake-Resistant Design," by H.B. Seed, C. Ugas and J. Lysmer - 1974 (PB 240 953)A03

EERC 74-13 "Earthquake Simulator Study of a Reinforced Concrete Frame," by P. Hidalgo and R.W. Clough - 1974 (PB 241 944)A13

EERC 74-14 "Nonlinear Earthquake Response of Concrete Gravity Dams," by N. Pal - 1974 (AD/A 006 583)A06

EERC 74-15 "Modeling and Identification in Nonlinear Structural Dynamics - I. One Degree of Freedom Models," by N. Distefano and A. Rath - 1974 (PB 241 548)A06

EERC 75-1 "Determination of Seismic Design Criteria for the Dumbarton Bridge Replacement Structure, Vol. I: Description, Theory and Analytical Modeling of Bridge and Parameters," by F. Baron and S.-H. Pang - 1975 (PB 259 407)A15

EERC 75-2 "Determination of Seismic Design Criteria for the Dumbarton Bridge Replacement Structure, Vol. II: Numerical Studies and Establishment of Seismic Design Criteria," by F. Baron and S.-H. Pang - 1975 (PB 259 408)A11 (For set of EERC 75-1 and 75-2 (PB 259 406))

EERC 75-3 "Seismic Risk Analysis for a Site and a Metropolitan Area," by C.S. Oliveira - 1975 (PB 248 134)A09

EERC 75-4 "Analytical Investigations of Seismic Response of Short, Single or Multiple-Span Highway Bridges," by M.-C. Chen and J. Penzien - 1975 (PB 241 454)A09

EERC 75-5 "An Evaluation of Some Methods for Predicting Seismic Behavior of Reinforced Concrete Buildings," by S.A. Mahin and V.V. Bertero - 1975 (PB 246 306)A16

EERC 75-6 "Earthquake Simulator Study of a Steel Frame Structure, Vol. I: Experimental Results," by R.W. Clough and D.T. Tang - 1975 (PB 243 981)A13

EERC 75-7 "Dynamic Properties of San Bernardino Intake Tower," by D. Rea, C.-Y. Liaw and A.K. Chopra - 1975 (AD/A008 406) A05

EERC 75-8 "Seismic Studies of the Articulation for the Dumbarton Bridge Replacement Structure, Vol. I: Description, Theory and Analytical Modeling of Bridge Components," by F. Baron and R.E. Hamati - 1975 (PB 251 539)A07

EERC 75-9 "Seismic Studies of the Articulation for the Dumbarton Bridge Replacement Structure, Vol. 2: Numerical Studies of Steel and Concrete Girder Alternates," by F. Baron and R.E. Hamati - 1975 (PB 251 540)A10

EERC 75-10 "Static and Dynamic Analysis of Nonlinear Structures," by D.P. Mondkar and G.H. Powell - 1975 (PB 242 434)A08

EERC 75-11 "Hysteretic Behavior of Steel Columns," by E.P. Popov, V.V. Bertero and S. Chandramouli - 1975 (PB 252 365)A11

EERC 75-12 "Earthquake Engineering Research Center Library Printed Catalog," - 1975 (PB 243 711)A26

EERC 75-13 "Three Dimensional Analysis of Building Systems (Extended Version)," by E.L. Wilson, J.P. Hollings and H.H. Dovey - 1975 (PB 243 989)A07

EERC 75-14 "Determination of Soil Liquefaction Characteristics by Large-Scale Laboratory Tests," by P. De Alba, C.K. Chan and H.B. Seed - 1975 (NUREG 0027)A08

EERC 75-15 "A Literature Survey - Compressive, Tensile, Bond and Shear Strength of Masonry," by R.L. Mayes and R.W. Clough - 1975 (PB 246 292)A10

EERC 75-16 "Hysteretic Behavior of Ductile Moment Resisting Reinforced Concrete Frame Components," by V.V. Bertero and E.P. Popov - 1975 (PB 246 388)A05

EERC 75-17 "Relationships Between Maximum Acceleration, Maximum Velocity, Distance from Source, Local Site Conditions for Moderately Strong Earthquakes," by H.B. Seed, R. Murarka, J. Lysmer and I.M. Idriss - 1975 (PB 248 172)A03

EERC 75-18 "The Effects of Method of Sample Preparation on the Cyclic Stress-Strain Behavior of Sands," by J. Mulilis, C.K. Chan and H.B. Seed - 1975 (Summarized in EERC 75-28)

EERC 75-19 "The Seismic Behavior of Critical Regions of Reinforced Concrete Components as Influenced by Moment, Shear and Axial Force," by M.B. Atalay and J. Penzien - 1975 (PB 258 842)A11

EERC 75-20 "Dynamic Properties of an Eleven Story Masonry Building," by R.M. Stephen, J.P. Hollings, J.G. Bouwkamp and D. Jurukovski - 1975 (PB 246 945)A04

EERC 75-21 "State-of-the-Art in Seismic Strength of Masonry - An Evaluation and Review," by R.L. Mayes and R.W. Clough 1975 (PB 249 040)A07

EERC 75-22 "Frequency Dependent Stiffness Matrices for Viscoelastic Half-Plane Foundations," by A.K. Chopra, P. Chakrabarti and G. Dasgupta - 1975 (PB 248 121)A07

EERC 75-23 "Hysteretic Behavior of Reinforced Concrete Framed Walls," by T.Y. Wong, V.V. Bertero and E.P. Popov - 1975

EERC 75-24 "Testing Facility for Subassemblages of Frame-Wall Structural Systems," by V.V. Bertero, E.P. Popov and T. Endo - 1975

EERC 75-25 "Influence of Seismic History on the Liquefaction Characteristics of Sands," by H.B. Seed, K. Mori and C.K. Chan - 1975 (Summarized in EERC 75-28)

EERC 75-26 "The Generation and Dissipation of Pore Water Pressures during Soil Liquefaction," by H.B. Seed, P.P. Martin and J. Lysmer - 1975 (PB 252 648)A03

EERC 75-27 "Identification of Research Needs for Improving Aseismic Design of Building Structures," by V.V. Bertero 1975 (PB 248 136)A05

EERC 75-28 "Evaluation of Soil Liquefaction Potential during Earthquakes," by H.B. Seed, I. Arango and C.K. Chan - 1975 (NUREG 0026)A13

EERC 75-29 "Representation of Irregular Stress Time Histories by Equivalent Uniform Stress Series in Liquefaction Analyses," by H.B. Seed, I.M. Idriss, F. Makdisi and N. Banerjee - 1975 (PB 252 635)A03

EERC 75-30 "FLUSH - A Computer Program for Approximate 3-D Analysis of Soil-Structure Interaction Problems," by J. Lysmer, T. Udaka, C.-F. Tsai and H.B. Seed - 1975 (PB 259 332)A07

EERC 75-31 "ALUSH - A Computer Program for Seismic Response Analysis of Axisymmetric Soil-Structure Systems," by E. Berger, J. Lysmer and H.B. Seed - 1975

EERC 75-32 "TRIP and TRAVEL - Computer Programs for Soil-Structure Interaction Analysis with Horizontally Travelling Waves," by T. Udaka, J. Lysmer and H.B. Seed - 1975

EERC 75-33 "Predicting the Performance of Structures in Regions of High Seismicity," by J. Penzien - 1975 (PB 248 130)A03

EERC 75-34 "Efficient Finite Element Analysis of Seismic Structure - Soil - Direction," by J. Lysmer, H.B. Seed, T. Udaka, R.N. Hwang and C.-F. Tsai - 1975 (PB 253 570)A03

EERC 75-35 "The Dynamic Behavior of a First Story Girder of a Three-Story Steel Frame Subjected to Earthquake Loading," by R.W. Clough and L.-Y. Li - 1975 (PB 248 841)A05

EERC 75-36 "Earthquake Simulator Study of a Steel Frame Structure, Volume II - Analytical Results," by D.T. Tang - 1975 (PB 252 926)A10

EERC 75-37 "ANSR-I General Purpose Computer Program for Analysis of Non-Linear Structural Response," by D.P. Mondkar and G.H. Powell - 1975 (PB 252 386)A08

EERC 75-38 "Nonlinear Response Spectra for Probabilistic Seismic Design and Damage Assessment of Reinforced Concrete Structures," by M, Murakami and J. Penzien - 1975 (PB 259 530)A05

EERC 75-39 "Study of a Method of Feasible Directions for Optimal Elastic Design of Frame Structures Subjected to Earthquake Loading," by N.D. Walker and K.S. Pister - 1975 (PB 257 781)A06

EERC 75-40 "An Alternative Representation of the Elastic-Viscoelastic Analogy," by G. Dasgupta and J.L. Sackman - 1975 (PB 252 173)A03

EERC 75-41 "Effect of Multi-Directional Shaking on Liquefaction of Sands," by H.B. Seed, R. Pyke and G.R. Martin - 1975 (PB 258 781)A03

EERC 76-1 "Strength and Ductility Evaluation of Existing Low-Rise Reinforced Concrete Buildings - Screening Method," by T. Okada and B. Bresler - 1976 (PB 257 906)A11

EERC 76-2 "Experimental and Analytical Studies on the Hysteretic Behavior of Reinforced Concrete Rectangular and T-Beams," by S.-Y.M. Ma, E.P. Popov and V.V. Bertero - 1976 (PB 260 843)A12

EERC 76-3 "Dynamic Behavior of a Multistory Triangular-Shaped Building," by J. Petrovski, R.M. Stephen, E. Gartenbaum and J.G. Bouwkamp - 1976

EERC 76-4 "Earthquake Induced Deformations of Earth Dams," by N. Serff and H.B. Seed - 1976

EERC 76-5 "Analysis and Design of Tube-Type Tall Building Structures," by H. de Clercq and G.H. Powell - 1976 (PB 252 220) A10

EERC 76-6 "Time and Frequency Domain Analysis of Three-Dimensional Ground Motions, San Fernando Earthquake," by T. Kubo and J. Penzien (PB 260 556)A11

EERC 76-7 "Expected Performance of Uniform Building Code Design Masonry Structures," by R.L. Mayes, Y. Omote, S.W. Chen and R.W. Clough - 1976

EERC 76-8 "Cyclic Shear Tests on Concrete Masonry Piers," Part I - Test Results," by R.L. Mayes, Y. Omote and R.W. Clough - 1976 (PB 264 424)A06

EERC 76-9 "A Substructure Method for Earthquake Analysis of Structure - Soil Interaction," by J.A. Gutierrez and A.K. Chopra - 1976 (PB 257 783)A08

EERC 76-10 "Stabilization of Potentially Liquefiable Sand Deposits using Gravel Drain Systems," by H.B. Seed and J.R. Booker - 1976 (PB 258 820)A04

EERC 76-11 "Influence of Design and Analysis Assumptions on Computed Inelastic Response of Moderately Tall Frames," by G.H. Powell and D.G. Row - 1976

EERC 76-12 "Sensitivity Analysis for Hysteretic Dynamic Systems: Theory and Applications," by D. Ray, K.S. Pister and E. Polak - 1976 (PB 262 859)A04

EERC 76-13 "Coupled Lateral Torsional Response of Buildings to Ground Shaking," by C.L. Kan and A.K. Chopra - 1976 (PB 257 907)A09

EERC 76-14 "Seismic Analyses of the Banco de America," by V.V. Bertero, S.A. Mahin and J.A. Hollings - 1976

EERC 76-15 "Reinforced Concrete Frame 2: Seismic Testing and Analytical Correlation," by R.W. Clough and J. Gidwani - 1976 (PB 261 323)A08

EERC 76-16 "Cyclic Shear Tests on Masonry Piers, Part II - Analysis of Test Results," by R.L. Mayes, Y. Omote and R.W. Clough - 1976

EERC 76-17 "Structural Steel Bracing Systems: Behavior Under Cyclic Loading," by E.P. Popov, K. Takanashi and C.W. Roeder - 1976 (PB 260 715)A05

EERC 76-18 "Experimental Model Studies on Seismic Response of High Curved Overcrossings," by D. Williams and W.G. Godden - 1976

EERC 76-19 "Effects of Non-Uniform Seismic Disturbances on the Dumbarton Bridge Replacement Structure," by F. Baron and R.E. Hamati - 1976

EERC 76-20 "Investigation of the Inelastic Characteristics of a Single Story Steel Structure Using System Identification and Shaking Table Experiments," by V.C. Matzen and H.D. McNiven - 1976 (PB 258 453)A07

EERC 76-21 "Capacity of Columns with Splice Imperfections," by E.P. Popov, R.M. Stephen and R. Philbrick - 1976 (PB 260 378)A04

EERC 76-22 "Response of the Olive View Hospital Main Building during the San Fernando Earthquake," by S. A. Mahin, R. Collins, A.K. Chopra and V.V. Bertero - 1976

EERC 76-23 "A Study on the Major Factors Influencing the Strength of Masonry Prisms," by N.M. Mostaghel, R.L. Mayes, R. W. Clough and S.W. Chen - 1976

EERC 76-24 "GADFLEA - A Computer Program for the Analysis of Pore Pressure Generation and Dissipation during Cyclic or Earthquake Loading," by J.R. Booker, M.S. Rahman and H.B. Seed - 1976 (PB 263 947)A04

EERC 76-25 "Rehabilitation of an Existing Building: A Case Study," by B. Bresler and J. Axley - 1976

EERC 76-26 "Correlative Investigations on Theoretical and Experimental Dynamic Behavior of a Model Bridge Structure," by K. Kawashima and J. Penzien - 1976 (PB 263 388)A11

EERC 76-27 "Earthquake Response of Coupled Shear Wall Buildings," by T. Srichatrapimuk - 1976 (PB 265 157)A07

EERC 76-28 "Tensile Capacity of Partial Penetration Welds," by E.P. Popov and R.M. Stephen - 1976 (PB 262 899)A03

EERC 76-29 "Analysis and Design of Numerical Integration Methods in Structural Dynamics," by H.M. Hilber - 1976 (PB 264 410)A06

EERC 76-30 "Contribution of a Floor System to the Dynamic Characteristics of Reinforced Concrete Buildings," by L.J. Edgar and V.V. Bertero - 1976

EERC 76-31 "The Effects of Seismic Disturbances on the Golden Gate Bridge," by F. Baron, M. Arikan and R.E. Hamati - 1976

EERC 76-32 "Infilled Frames in Earthquake Resistant Construction," by R.E. Klingner and V.V. Bertero - 1976 (PB 265 892)A13

UCB/EERC-77/01 "PLUSH - A Computer Program for Probabilistic Finite Element Analysis of Seismic Soil-Structure Interaction," by M.P. Romo Organista, J. Lysmer and H.B. Seed - 1977

UCB/EERC-77/02 "Soil-Structure Interaction Effects at the Humboldt Bay Power Plant in the Ferndale Earthquake of June 7, 1975," by J.E. Valera, H.B. Seed, C.F. Tsai and J. Lysmer - 1977 (PB 265 795)A04

UCB/EERC-77/03 "Influence of Sample Disturbance on Sand Response to Cyclic Loading," by K. Mori, H.B. Seed and C.K. Chan - 1977 (PB 267 352)A04

UCB/EERC-77/04 "Seismological Studies of Strong Motion Records," by J. Shoja-Taheri - 1977 (PB 269 655)A10

UCB/EERC-77/05 "Testing Facility for Coupled-Shear Walls," by L. Li-Hyung, V.V. Bertero and E.P. Popov - 1977

UCB/EERC-77/06 "Developing Methodologies for Evaluating the Earthquake Safety of Existing Buildings," by No. 1 - B. Bresler; No. 2 - B. Bresler, T. Okada and D. Zisling; No. 3 - T. Okada and B. Bresler; No. 4 - V.V. Bertero and B. Bresler - 1977 (PB 267 354)A08

UCB/EERC-77/07 "A Literature Survey - Transverse Strength of Masonry Walls," by Y. Omote, R.L. Mayes, S.W. Chen and R.W. Clough - 1977

UCB/EERC-77/08 "DRAIN-TABS: A Computer Program for Inelastic Earthquake Response of Three Dimensional Buildings," by R. Guendelman-Israel and G.H. Powell - 1977 (PB 270 693)A07

UCB/EERC-77/09 "SUBWALL: A Special Purpose Finite Element Computer Program for Practical Elastic Analysis and Design of Structural Walls with Substructure Option," by D.Q. Le, H. Peterson and E.P. Popov - 1977 (PB 270 567)A05

UCB/EERC-77/10 "Experimental Evaluation of Seismic Design Methods for Broad Cylindrical Tanks," by D.P. Clough

UCB/EERC-77/11 "Earthquake Engineering Research at Berkeley - 1976," - 1977

UCB/EERC-77/12 "Automated Design of Earthquake Resistant Multistory Steel Building Frames," by N.D. Walker, Jr. - 1977

UCB/EERC-77/13 "Concrete Confined by Rectangular Hoops Subjected to Axial Loads," by D. Zallnas, V.V. Bertero and E.P. Popov - 1977

UCB/EERC-77/14 "Seismic Strain Induced in the Ground During Earthquakes," by Y. Sugimura - 1977

UCB/EERC-77/15 "Bond Deterioration under Generalized Loading," by V.V. Bertero, E.P. Popov and S. Viwathanatepa - 1977

UCB/EERC-77/16 "Computer Aided Optimum Design of Ductile Reinforced Concrete Moment Resisting Frames," by S.W. Zagajeski and V.V. Bertero - 1977

UCB/EERC-77/17 "Earthquake Simulation Testing of a Stepping Frame with Energy-Absorbing Devices," by J.M. Kelly and D.F. Tsztoo 1977

UCB/EERC-77/18 "Inelastic Behavior of Eccentrically Braced Steel Frames under Cyclic Loadings," by C.W. Roeder and E.P. Popov - 1977

UCB/EERC-77/19 "A Symplified Procedure for Estimating Earthquake-Induced Deformations in Dams and Embankments," by F.I. Makdisi and H.B. Seed - 1977

UCB/EERC-77/20 "The Performance of Earth Dams during Earthquakes," by H.B. Seed, F.I. Makdisi and P. de Alba - 1977

UCB/EERC-77/21 "Dynamic Plastic Analysis Using Stress Resultant Finite Element Formulation," by P. Lukkunapvasit and J.M. Kelly 1977

UCB/EERC-77/22 "Preliminary Experimental Study of Seismic Uplift of a Steel Frame," by R.W. Clough and A.A. Huckelbridge - 1977

UCB/EERC-77/23 "Earthquake Simulator Tests of a Nine-Story Steel Frame with Columns Allowed to Uplift," by A.A. Huckelbridge - 1977

UCB/EERC-77/24 "Nonlinear Soil-Structure Interaction of Skew Highway Bridges," by M.-C. Chen and Joseph Penzien - 1977

UCB/EERC-77/25 "Seismic Analysis of an Offshore Structure Supported on Pile Foundations," by D.D.-N. Liou - 1977

UCB/EERC-77/26 "Dynamic Stiffness Matrices for Homogeneous Viscoelastic Half-Planes," by G. Dasgupta and A.K. Chopra - 1977

UCB/EERC-77/27 "A Practical Soft Story Earthquake Isolation System," by J. M. Kelly and J. M. Eidinger - 1977

UCB/EERC-77/28 "Seismic Safety of Existing Buildings and Incentives for Hazard Mitigation in San Francisco: An Exploratory Study," by A. J. Meltsner - 1977

UCB/EERC-78/01 "The Development of Energy-Absorbing Devices for Aseismic Base Isolation Systems," by J. M. Kelly and D. F. Tsztoo - 1978